# Thermoelectricity for IoT – a review

Maciej Haras, Thomas Skotnicki

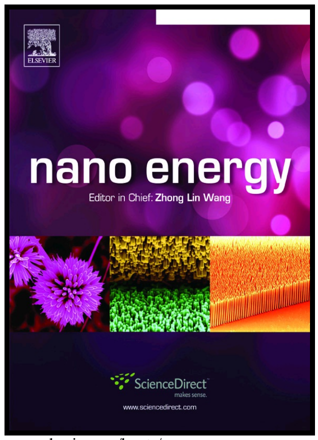


www.elsevier.com/locate/nanoenergy

PII: S2211-2855(18)30728-6
DOI: https://doi.org/10.1016/j.nanoen.2018.10.013
Reference: NANOEN3091

To appear in: *Nano Energy*

Received date: 3 August 2018
Revised date: 5 October 2018
Accepted date: 5 October 2018

Cite this article as: Maciej Haras and Thomas Skotnicki, Thermoelectricity for IoT – a review, *Nano Energy,* https://doi.org/10.1016/j.nanoen.2018.10.013

# Thermoelectricity for IoT – a review

Maciej Haras[1], Thomas Skotnicki[1,2]

[1]Warsaw University of Technology, Centre for Advanced Materials and Technologies CEZAMAT, ul. Poleczki 19, 02-833 Warsaw, Poland

[2]Warsaw University of Technology, Faculty of Electronics and Information Technology, Institute of Microelectronics and Optoelectronics, ul. Koszykowa 75, 00-662 Warsaw, Poland

M.Haras@cezamat.eu

skotnicki.cezamat@gmail.com

Abstract

We are witnessing an unprecedented expansion of Internet of Things (IoT) market, whose nodes are already outnumbering human population several times. Despite the huge popularity of IoT, its further expansion is slowed down by a lack of viable power supply methods capable to replace wires or batteries. Due to IoT demand for alternative supply, energy harvesting (EH) gathers attention from scientific groups all around the world. In particular, thermoelectricity (TE) seems to be a natural and intuitive candidate for IoT owing to magnitude and omnipresence of heat losses and amenability to direct, vibrationless, noiseless and reliable conversion. This review provides up-to-date comparison and evaluation of a recent progress in the field of thermoelectricity, resulting primarily from multidisciplinary optimization of materials, topologies and controlling circuitry. The improvement in materials integrates two trends: nanostructural modulation of pre-existing, conventional thermoelectric materials and synthesis of novel ones. Regarding topology, TE responds better and better to miniaturization trend of semiconductor industry, driven by miniaturization trend, by proposing alternatives to conventional π-type topology. And finally, recently developed controlling circuits consume extremely low power while idle, exhibit above-90% efficiency and start-up with ultra-low input voltages. Combined, these improvements position TE closer to marketization than ever before.

Graphical abstract

fx1

Introduction

Urged by the worldwide increasing demand in energy [1,2] (*see Fig. 1*a), constrained by the limited reserves of fossil fuels [2–5] (*see Fig. 1*a) and facing a problem of global climate change [6–9] (*see Fig. 1*b), all innovative solutions contributing to improve the renewable production of energy are playing a strategic role. As presented in Fig. 1a, the natural reserves of fossil fuels are predicted to be exhausted within: next 50 years for oil [5,10] and more than 100 years for coal [2,4], gas [2,3], and nuclear [11]. In this context, searching for alternative energy sources is an urgent necessity. If we target today a fully connected and ***I***nternet ***o***f ***T***hings (***IoT***) controlled planet, we cannot expose this strategy to a total failure in 50-100 years due to fossil energy shortage.

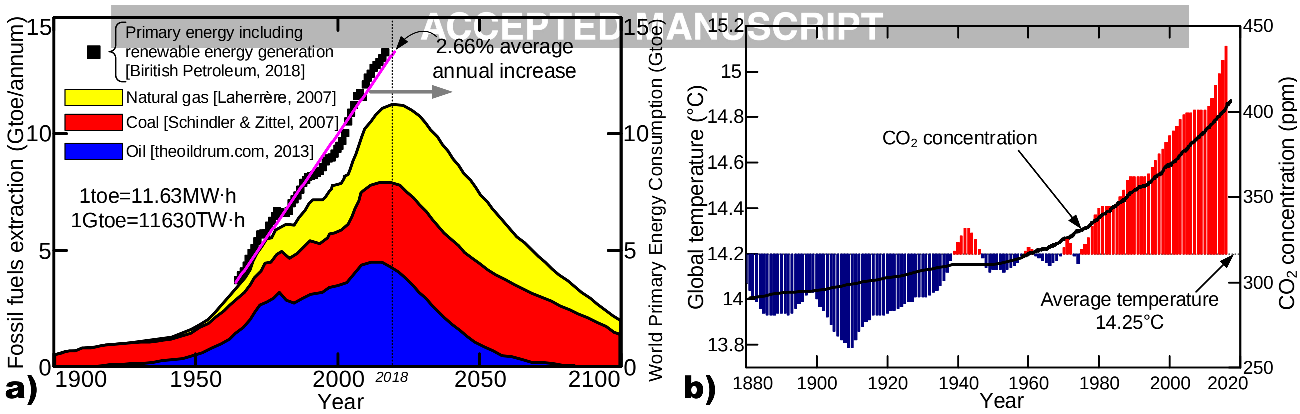


Fig. 1**a)** Global fossil fuels historical extraction and reserves forecasts [2–5] superposed with primary energy consumption [1,2]; **b)** historical evolution of annual mean temperature [6,7,9] and $CO_2$ concentration in atmosphere [8]

Meanwhile, an emerging market of ***IoT*** expands at a rate never seen before [12]. The energy consumed by an ***IoT*** node counts in ~0.86kW·h/annum (*supposing 100μJ per cycle to be repeated every second, see further*) – 13 decades behind the world electricity consumption as high as 25.5 TW·h in 2017 [2]. Nevertheless, if we take into account the prospected count of ***IoT*** nodes (*tens of trillions in 50-100 year perspective*), the total energy consumption by ***IoT*** may also reach the level of 8.6 TW·h/annum, becoming on the same order of magnitude. This clearly indicated the necessity of supplying ***IoT*** with harvested rather than fossil energy. ***IoT*** principle is to establish communication between devices (*Things*) omitting human intervention. Basing on this principle countless number of applications are realized *e.g.* smart city [13], remote health care [14,15], fully automated production lines [16,17] *etc.* Topological particularity of ***IoT*** systems lies in their pyramidal structure [13,18]. A conventional ***IoT*** system consists of numerous communicating nodes (*also called leafs*) which are monitoring particular parameters, such as temperature, presence, light density, traffic intensity *etc.* measured data are temporarily transmitted to the overriding unit (*see Fig. 2a*). Supervising unit stores and analyses data and reacts appropriately. Historically, ***IoT*** systems first emerged in the military and entered into the civil market owing to a concept of *Intelligent buildings* [19] and subsequently got popularized [20–22].



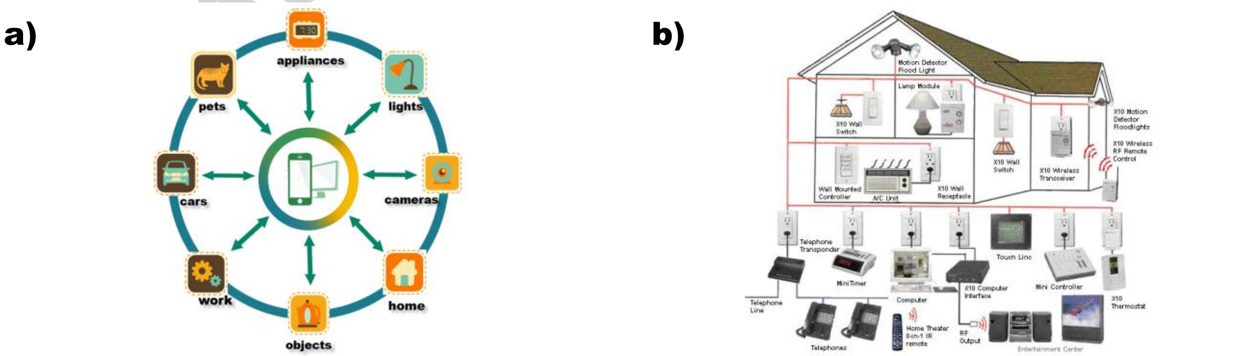


*Fig. 2**a)** Schematic illustration of communication chain in the **IoT** system; **b)** Example of installation in the intelligent building*

An endless list of ***IoT*** applications is reflected by a rapidly rising number of ***IoT*** nodes and by growing market penetration by ***IoT*** devices (see *Fig. 3*a). At present, there are ~5 ***IoT*** nodes per each human and this proportion will be doubled in the next 4-5 years. It is too early to judge, but in the next 50-100 year perspective, the count of ***IoT*** nodes may reach tens of trillions devices. Quickly expanding ***IoT*** market has significant societal impact, creating considerable employment growth (*see* Fig. 3*b*). At the end of 2018 the number of created jobs is forecasted to reach almost 3 million and is predicted to further rise up to 5 million within next two years. From this perspective, the ***IoT*** market is of a huge social importance. Significantly, this sizable employment market built up within less than a decade – a speed that has no precedence.

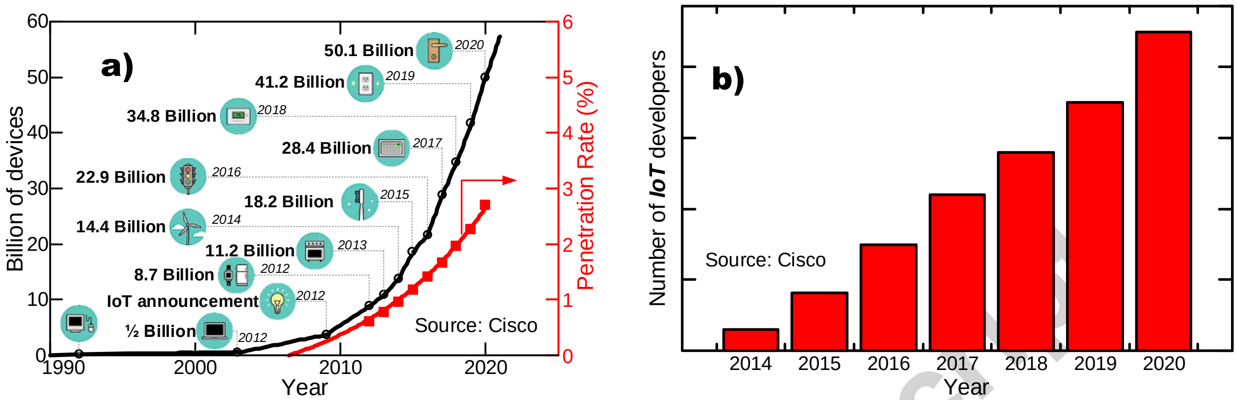


*Fig. 3**a)** Predictive count and penetration rate of IoT devices [12]; **b)** Forecasted employment in the IoT and Year-on-Year IoT devices quantity rise [12]*

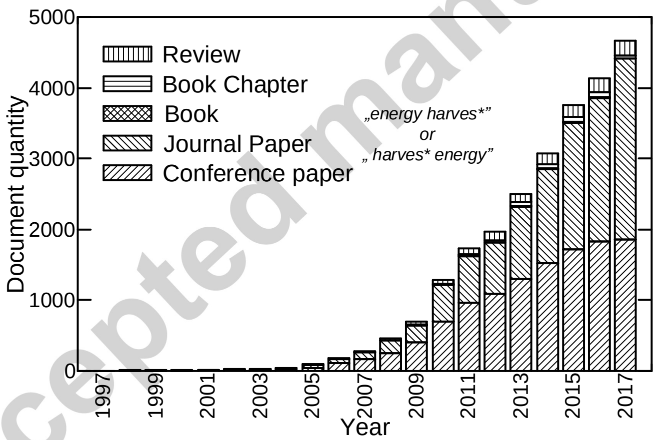


*Fig. 4 Historical count of energy harvesting publications. From the Scopus browser for "energy harves*" or "harves* energy" query.*

The ***IoT*** expansion on the market could proceed even faster but it is significantly hampered by a lack of economically attractive and energetically efficient alternatives for powering ***IoT*** nodes. Production of useful energy from omnipresent or lost energy is called the ***E***nergy ***H***arvesting (***EH***). ***EH*** can be a huge relief for ***IoT*** allowing its further expansion through construction of wire/battery free devices so needed by the ***IoT***. That is why ***EH*** gathers remarkable attention from scientific community, evidenced by clear acceleration in this field (*see Fig. 4*). Within the period of last 10 years the number of publications per year increased close to 20 times.

# 1. NEW PARADIGM FOR ENERGY GENERATION DUE TO IOT

In the field of ***IoT*** we more often speak of energy harvesting than on generation. This is due to smaller energy consumption that coms to play. Between the consumption levels in ***IoT*** applications ($\mu J$) and those in dwelling/industrial ($MJ$) we have 12 orders of magnitude difference. Therefore, regarding ***IoT*** we rather speak of ***E***nergy ***H***arvesting (***EH***) (*minute, free energy from environment*) than generation.

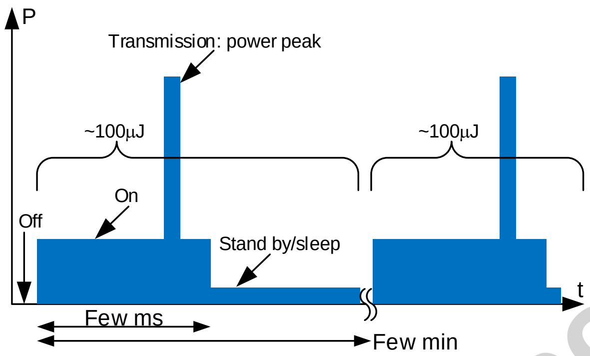


*Fig. 5 Intermittent energy consumption by a GreenNet IoT node from STMicroelectronics. Note peaks of transmission as the most demanding moments energy-wise [23]*

Although a typical power consumption of a single ***IoT*** node is very small (*see Fig. 5*), it is difficult to satisfy. Wiring the nodes is undesirable, considering their quantity, size and portability. Usage of batteries is impractical as well as wiring them. Firstly, an access to nodes is quite often very difficult (*for example, in harsh industrial environment*). Secondly, replacing or checking batteries in tenths of billions of communicating *Things* would occupy all global population. Thirdly, powering nodes using lithium-based batteries is also undesirable considering environmental impact.

Therefore, the ***IoT*** expansion is to large extend blocked by a lack of efficient and reliable alternatives to batteries to supply the communicating nodes. Autonomously supplied nodes would be a huge relief from the environmental, economic and practical standpoint not only for ***IoT*** but for the whole semiconductor industry.

A typical ***IoT*** node (*intelligent sensor*) works in an intrinsically discontinuous fashion. It repeatedly performs a set of actions, such as measuring a parameter followed by processing the acquired information, coding it and transmitting the result wirelessly. It does all that in milliseconds and then gets idle for some time (*often for minutes or even longer, see Fig. 5*). It is thus more adequate to focus on the amount of energy needed for a singular set of actions than on the continuous power consumption. Typically, the needs of an ***IoT*** node may be satisfied even by a very weak power source that is gradually filling an energy storage element (*e.g. a capacitor*) and the node will activate only when having stored enough energy for a single act of sensing, information treatment, and transmission. An advanced ***IoT*** node needs less than 100µJ for that. Such a low energy requirement opens up the possibility to exploit a concept of energy harvesting to power the nodes [24–26]. This approach relies on converting omnipresent, lost energy into a useful electrical energy and has a potential to unlock ***IoT*** expansion on the market. It is to be emphasized that this means a new paradigm in supplying electronics circuits composing ***IoT***. Instead of continuous powering, well described in Watt, (*as for conventional circuits*) it is more appropriate to speak of discontinuous energy portions (*see Fig. 5*), well described in Joule, needed for each operation cycle in the intermittent functioning of ***IoT***.

In the following a detail regard on the availability and abundance of macro- and micro-scale source energies exploitable by energy harvesting.

# 2. ENERGY SOURCE AVAILABILITY

***EH*** can be considered as a branch of technology developing devices able to convert an ambient energy into a useful energy (*usually electric one*). Two classes/types of ***EH*** can be distinguished: (i) macro-scale harvesting , considered usually as a renewable source of energy [27–29] and (ii) micro-scale harvesting, mainly converting waste energy [25,26]. It is worth noting that majority of micro-scale ***EH*** techniques have also macro-scale counterparts. Of course we will focus on micro-scale ***EH*** in this paper, but we need to realize that if micro-scale ***EH*** is a commodity today (*alternative exists*) it may become a necessity tomorrow, due to depletion of fossil energy reserves.

Our planet offers multiple possibilities for micro-scale harvesting. As illustrated in Table 1, there is an enormous gap between available energies for natural sources and theirs useful exploitation. This unexploited reserves can thus be used as inputs for ***EH*** to power ***IoT***.

*Table 1 Global resources in renewable energy and the energy currently available*

| Energy source | Global resources (TW) | Currently available (TW) | Percentage of used global resources (%) |
|---|---|---|---|
| **Wind** | **1700**[a] | **0.539**[b] | **0.032** |
| **Geothermal** | **45**[a] | **0.0128**[b] | **0.028** |
| **Hydroelectric** | **1.9**[a] | **1.114**[b] | **58.63** |
| **Solar Photovoltaic** | **6500**[a] | **0.402**[b] | **0.006** |
| **Concentrators of Solar Thermal Power (CSP)** | **4600**[a] | **0.0049**[b] | **0.0001** |

[a] Data based on [30]

[b] Data based on [1]

However, except for hydroelectric sources, the current exploitation of renewables is miserable, despite of a clear necessity, technological feasibility and huge unused reserves that could be allocated. In every-day life, these losses take various forms, Fig. 6 shows micro-harvesting possibilities in domestic environment along with their power densities. Analysis of Fig. 6 leads to conclusions similar to the ones emerging from Table 1. Firstly, domestic environment is rich in various energy losses. Secondly, lost energy power densities are covering very wide range up to 125mW/cm$^2$ for waste heat. Less powerful sources like radiofrequency waves can provide up to 1.5μW/cm$^2$ in dense urban zones. Importantly, the presented power densities are typical and in extreme situations can be exceeded. Finally, our ordinary existence is accompanied by losses continuously, dwellings and offices are places where these losses are concentrated.

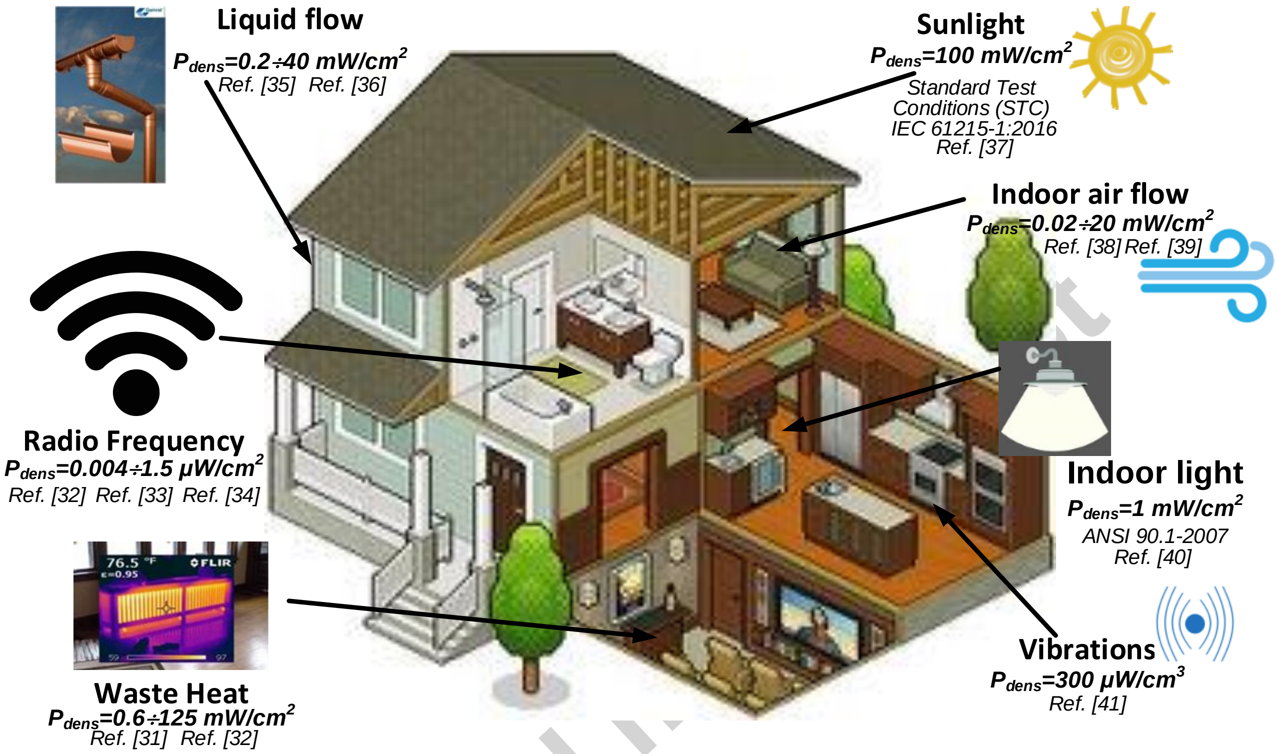


*Fig. 6 Evaluation of available power densities from given sources in domestic environment based on: thermal - [31,32]; radio frequency - [32–34]; liquid flow - [35,36]; sunlight - [37]; indoor air flow - [38,39] indoor light - [40]; vibrations - [41]*

Progressing miniaturization and performance boost opens new possibilities for energy harvesting, on this background even a human body becomes a source of harvestable energy. Fig. 7 evaluates power loss due to human activities. Human body provides mainly mechanical energy in form of movements (*breathing, walking, etc.*) and thermal energy linked to body heat. The most of this energy is generated by legs and arms movements and it could in principle meet all needs of micro-power devices. Considering that mankind population exceeds 7 billion [42] and continues to grow, the prospect to produce small amounts of useful energy from everyday human activities seems very attractive.

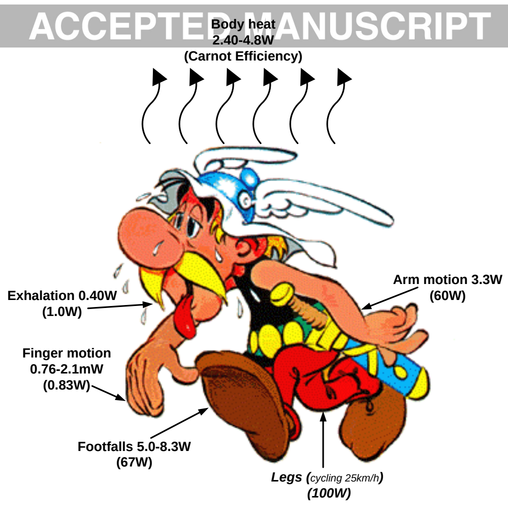


*Fig. 7 Average available energy from different human activities [43]*

Finally, it can be concluded that energy losses are inevitably accompanying our ordinary life activities, being thus omnipresent. Among various types of losses, the heat losses are the biggest.

# 3. ENERGY HARVESTING – METHODS

Renewable energy can be harvested in two ways: (i) on macro scale exploiting Nature-provided renewable energy sources *e.g. wind, hydroelectric, geothermal etc.* and (ii) on micro scale by reusing energy losses resulting from human-driven activities. The macro harvesting is offering access to attractive and sizable reserves and can be a salvation from greenhouse effect and depleting fossils fuels. The micro-scavenging opens a prospect for autonomous, battery/wires-free devices vitally needed for developing the market of ***IoT*** and the whole semiconductor industry.

Taking advantage of various energy losses requires diverse ***EH*** techniques. A taxonomy of ***EH*** techniques accounting for the source of energy and harvester's physical background [44] is depicted in Fig. 8. It is important to note that classified ***EH*** techniques from Fig. 8 are able to produce enough energy to supply various electronic devices, Fig. 9 links typical consumed power for various electronic devices with different energy harvesting techniques. It can be concluded that energy harvesting can provide sufficient supply for very wide range of electronic equipment.

Often in real life different types of losses (*e.g. light and heat or vibrations and heat etc.*) occur at the same place and time. Optimal use of this situation requires integration of at least two energy harvesters into one device, that is called hybridization. Hybrid energy harvesters are very popular due to enlargement of their application field and significant performance boost. Classifying hybrid harvesters can be done by naming different effects they are using (*e.g.* ***PZ***+***EM*** *or* ***TE***+***PV***). Among classic hybrid energy harvester, the fusion of ***PZ*** with ***EM*** is one of the easiest to achieve and thus this hybridization is the most popular [45–49]. Other interesting examples of hybrid harvesters are ***EM***+***TRE*** [50–53], ***PZ***+***TRE*** [54,55]. Integration of more than two harvesting methods into one device has many examples in the literature [56–62]. More information on hybrid energy harvester can be found in [63] chapter 2. 

Motivated by significant progress in the field, aforementioned amount of heat losses and real need for alternative supply for ***IoT***, this review is focused on ***T***hermo***E***lectric (***TE***) ***EH***.

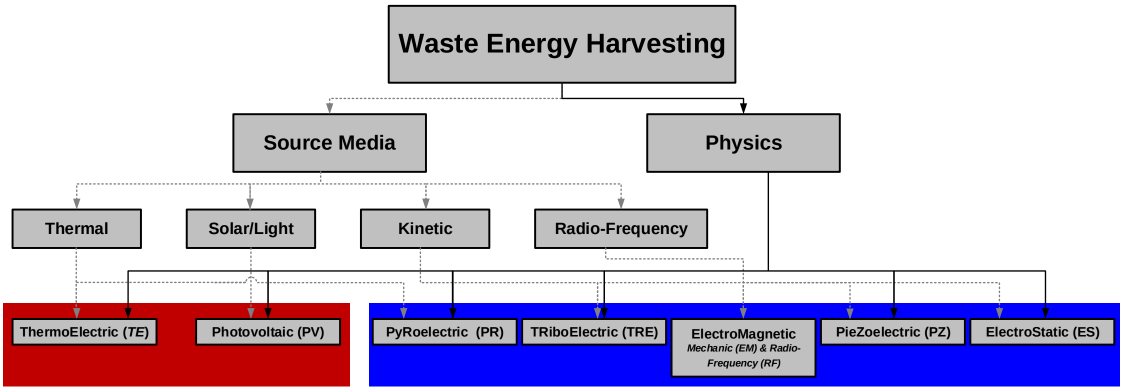


*Fig. 8 Taxonomy of waste energy harvesting techniques classified per source energy and physical phenomena [44]*

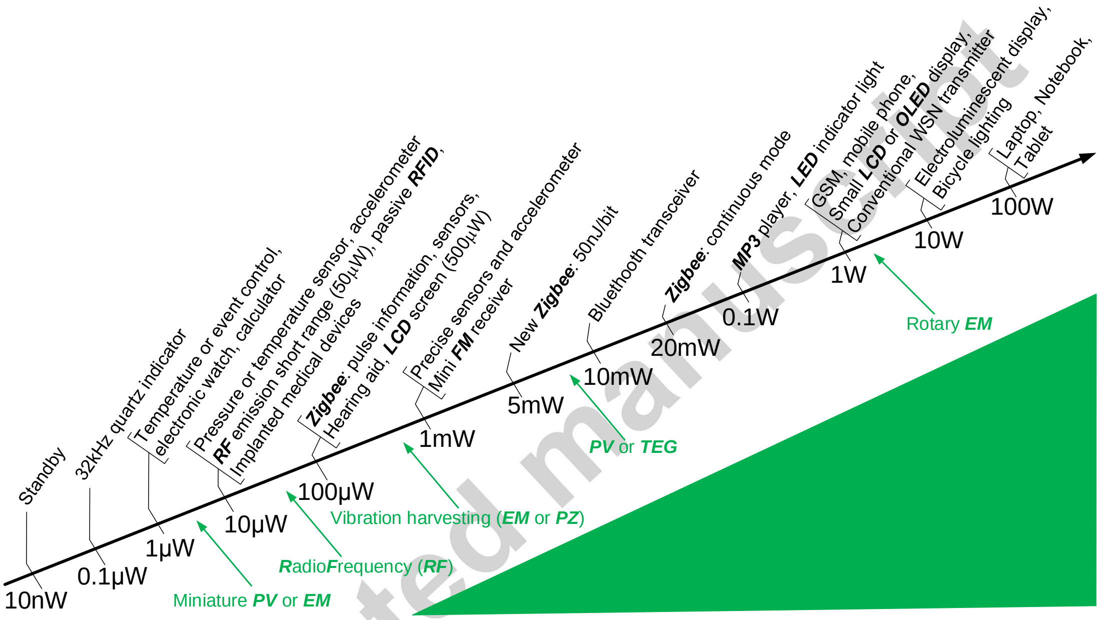


*Fig. 9 Harvested power for different scavenging technologies and corresponding electric power consumption for given devices [64], [65], [66], [67].*

# 4. THERMOELECTRICITY TOPOLOGICAL ASPECTS

As the most difficult to conserve, the heat energy exhibits the highest losses. Quantitatively, approximately half of heat energy is dissipated to atmosphere [68]. ***USA*** industry releases almost 30% of input energy in a form of heat each year [69].

Huge heat losses can be at least partially recovered using the ***T***hermo***E***lectric (***TE***), ***TR***ybo***E***lectric (***TRE***) or ***P***y***R***oelectric (***PR***) [70–72] effects or by hybridization of one of them with other harvesting methods. Although ***TE*** and ***PR*** are both converting heat into electricity the conversion mechanism is completely different. ***PR*** is an ability of certain materials to generate temporary voltage when heated or cooled. In contrast with ***TE***, where temperature gradient is needed, ***PR*** generates voltage remaining isothermal, requiring temperature changes in time. In this review focus is put on ***TE*** effect. It was discovered in 1821 by T. Seebeck [73], it transforms heat into electricity in silent, direct, vibrationless, and extremely reliable way [74]. Thanks to those advantages thermoelectricity found applications in hard to reach locations, *e.g.* in spaceships [75–77], in medicine [78,79], in transportation industry [76,80–82]. Efficient usage of ***TE*** effect is possible in ***T***hermo***E***lectric ***G***enerator (***TEG***) topology exclusively designed for this purpose and summarized in Fig. 10. Conventional π-type topology is depicted in Fig. 10a [83]. It consists of two vertical pillars metallically strapped on top, while the temperature is distributed from top to the bottom. ***TE*** effect principle is illustrated in Fig. 10b, majority carriers (*electrons* ($e^-$) *or holes* ($h^+$)) located at the hot site are migrating towards colder site. This results in unbalanced carrier's density and thermally-induced voltage formation ($V_N$ *and* $V_P$). This topology arranges thermocouple in parallel for heat and in series for current thus boosting the output voltage ($V_{TOT}$).

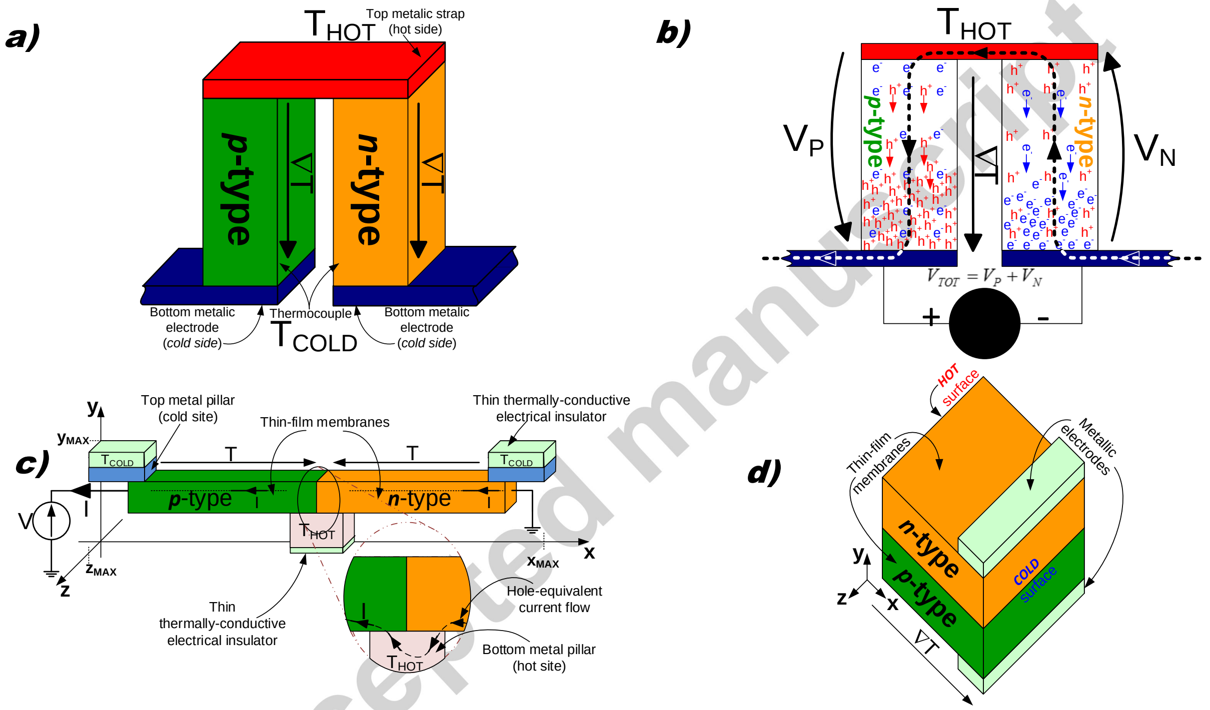


*Fig. 10 Thermoelectric generators topologies* ***a)*** *π-type;* ***b)*** *thermally-induced voltage formation ($h^+$ states for hole and $e^-$ for electron) dotted line presents current flow through the generator;* ***c)*** *lateral;* ***d)*** *large area pn junction.*

Nowadays engineers are confronted with demand to continually improve performance, miniaturize size and reduce price of electronic devices. On this background, the π-type topology (*Fig. 10a*) is difficult to integrate and thus a planar version of ***TEG*** has been proposed (*Fig. 10*c) [84–88]. Apart from being more adapted to the requirements of digital industry it can integrate additional properties *e.g.* mechanical flexibility. Another ***TEG*** topology that responds to aforementioned industrial miniaturization trend is a large area *pn* junction Fig. 10d [89–93]. This is a very simple structure consisting of two oppositely doped regions and two metallic electrodes placed in cold area for power extraction. An advantage of this topology is its simple and cheap fabrication. Additional information about topological progress in thermoelectricity is provided in [94].

Further boosting of ***TEG***s performance resulted from topological alternatives *e.g.* multistage generators [95–97], segmented thermocouples arrangement [98–101] or foil/film generators [102–105]. Those ***TEG***s are derived from structures depicted in Fig. 10, thus can be considered as various versions of a given topologies.

# 5. THERMOELECTRICITY - MATERIAL ASPECTS

Despite of the advantages of ***TE*** effect and a widespread availability of heat losses, it took more than 100 years for the first ***TEG*** to be installed [106]. This gap between the discovery and its technological exploitation was caused by a lack of thermoelectrically efficient and economically viable materials. ***TE*** is a single-step conversion which of performance and attractiveness relies mainly on the material which is executing this conversion. Evaluation of a thermoelectric performance of a given material is usually done using a non-dimensional-figure-of-merit (***zT***) (*Eq. 1*) [107] which reflects the conversion efficiency ($\eta_{TE}$) (*Eq. 2*) [108] being a fraction of Carnot limit ($\eta_{Carnot}$) Eq. 3.

$$zT = \frac{\sigma \cdot S^2}{\kappa} \cdot T = \frac{\sigma \cdot S^2}{\kappa_{el} + \kappa_{ph}} \cdot T \qquad \textit{Eq. 1}$$

$$\eta_{TE} = \left(1 - \frac{T_{COLD}}{T_{HOT}}\right) \cdot \frac{\sqrt{1+zT} - 1}{\sqrt{1+zT} + \frac{T_{COLD}}{T_{HOT}}} \qquad \textit{Eq. 2}$$

$$\eta_{Carnot} = 1 - \frac{T_{COLD}}{T_{HOT}} \qquad \textit{Eq. 3}$$

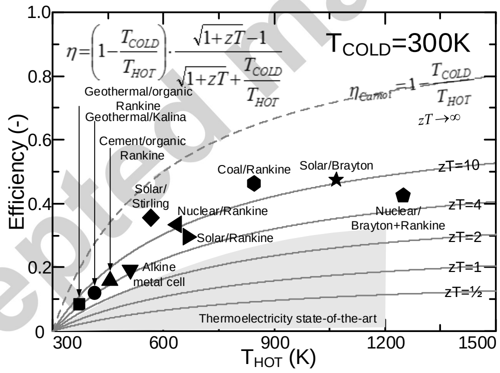


*Fig. 11 Conversion efficiency for different zT values over temperature; dots are pointing the common efficiency for conventional energy conversion engines in different energy cycles highlight corresponds to attainable currently thermo-generator's efficiencies [109–111]*

Typically ***TEG*** operates in externally imposed thermal conditions that leads to a situation when $\eta_{TE}$ can be improved only through the use of materials with higher ***zT***. Benchmarking of $\eta_{TE}$ with conventional energy conversions is depicted in Fig. 11 [109–111].

Good thermoelectric should converge towards the so-called phonon-glass/electron-crystal (***PGEC***) [112] limit and thus should integrate antagonistic properties: (i) high crystal-like electric conductivity ($\sigma$), (ii) low glass-like thermal conductivity ($\kappa = \kappa_{el} + \kappa_{ph}$) and (iii) as high as possible thermopower (***S***), see Fig. 12. Electric conductivity exhibits linear dependence on carrier density (***n***) as is a product of ***q***-elementary charge, carrier mobility ($\mu$) and ***n*** ($\sigma = q \cdot \mu \cdot n$). Thermal conductivity is a sum of two contributions dominating lattice ($\boldsymbol{\kappa}_{ph}$=$L_{ph}\cdot V_s\cdot C_v/3$) related to heat propagation through phonons, depending on mean-free path ($L_{ph}$), sound velocity ($V_s$) and heat capacity ($C_v$), and negligible electronic ($\boldsymbol{\kappa}_{el}$=$L_0\cdot\boldsymbol{\sigma}\cdot T$) where $L_0$=2.45×$10^{-8}$ $V^2/K^2$ is Lorentz constant, representing heat propagation with charged carriers [113]. ***S*** can be understood as entropy per carrier or heat per carrier over temperature [114,115]. In other words ***S*** can be thought as an ability of free carriers to perform thermally-induced migration from hot towards cold temperature. Metals have small ***S*** which can be explained by high density of free carriers, due to carrier-to-carrier scattering the thermally-induced migration towards colder regions is very small. In contrast insulators, exhibit high ***S***, since low carrier density facilitates thermally-induced movement of carriers from hot towards cold region. The above discussion is graphically summarized in Fig. 12 presenting ***S***, $\boldsymbol{\sigma}$ and $\boldsymbol{\kappa}$ as function of carrier density. Insulators have big ***S*** and usually low $\boldsymbol{\kappa}$ however their poor electronic transport properties are dramatically lowering ***zT***. Metals exhibit fantastic $\boldsymbol{\sigma}$ but their crystal structure results in very high $\boldsymbol{\kappa}$ additionally large carrier concentration results in low ***S***. Semiconductors are offering optimal compromise between ***S***, $\boldsymbol{\sigma}$, and $\boldsymbol{\kappa}$ resulting in the highest ***zT*** and defining them as best materials for thermoelectricity.

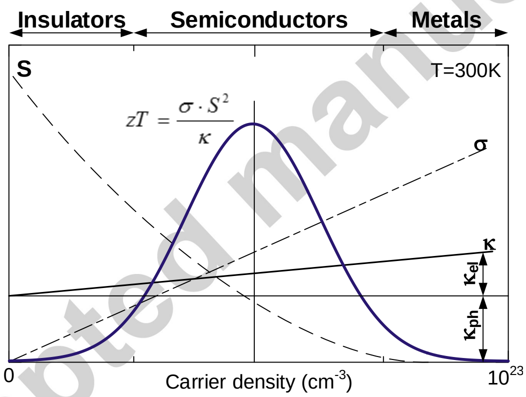


*Fig. 12 Thermopower (**S**), electrical conductivity (σ), thermal conductivity (κ) and zT versus carrier density [116]*

Optimization of ***zT*** is very difficult since $\boldsymbol{\kappa}$, $\boldsymbol{\sigma}$ and ***S*** are interdepended. Thus it took more than 30-years to develop material with ***zT***>1 [117] (*see Fig. 15*). Scientists seeking for good thermoelectrics adopted two different approaches: (i) boosting ***zT*** of conventional thermoelectric materials using nanostructuration (*see Fig. 13a*), and (ii) synthesis of new thermoelectrically efficient materials (*e.g. skutterudites, clathrates etc. see Fig. 13b*). Significant ***zT*** improvement can be obtained by phonon scattering amplification which in practice can be achieved by placing large, heavy and metallic atoms inside the unit cell. Such unit cell structure have a lot of void spaces which creates disorder in phonon propagation throughout the material and reduces lattice thermal conductivity ($\boldsymbol{\kappa}_{ph}$) [118]. High ***zT*** of skutterudites [119] and clathrates [120] is achieved owing to such structure.

From practical standpoint synthesis of thermoelectric materials, especially modern, constitutes ambitious, expensive and complex challenge. Huge diversity of technological processes used for thermoelectric compounds synthesis makes a brief review very difficult. A majority of thermoelectrics are fabricated using: (i) ball-milling, (ii) hydrothermal synthesis, (iii) melt spinning, (iv) hot- and cold-pressing, (v) spark plasma and thermal sintering and (vi) chemical methods, detailed list of material synthesis methods can be found in [121] Table 1.1. In practice most of clathrates are synthetized by thermal sintering of all elements above melting temperature. To increase composition uniformity, sintering takes several hours and the sample vibrates during this process. After sintering a material has to be densified/cooled which is challenging, since usually high-temperature sintering is used a relaxation of thermally induced mechanical stress can lead to defect formation [122]. Despite that skutterudites have crystalline structure similar to clathrates their fabrication is completely different. Synthesis of $Yb_{0.19}Co_4Sb_{12}$-skutterudite requires mixing all including elements which is usually done by ball milling technique, followed by hot pressing densification usually in the atmosphere of neutral gas [123,124]. High-***zT*** compounds of SnSe [125] are synthetized using special thermal treatment involving high-temperature soaking for several hours, followed by high-temperature crystal growth.

Nanostructuration and new material synthesis are continually boosting ***zT*** and it is at present impossible to judge neither which trend is dominant nor which one will shape thermoelectricity in the future. Nanostructuration (*Fig. 13*a) can be more attractive for industry, since it boosts ***zT*** of well-known conventional materials thus imposing moderate modifications of production lines, insuring technological compatibility and allowing full monolithic integration on-chip [126–130]. Nanostructuration can also additionally rise ***zT*** of recently discovered bulk thermoelectrics (*see Fig. 13*b). Fig. 14 illustrates nanostructurally-induced ***zT*** improvement for chosen materials. On the other hand progress in bulk thermoelectrics (*Fig. 13b*) converges mostly towards complex and expensive materials usually having sophisticated synthesis but offering fantastic ***zT*** values. Moreover, practical construction of ***TEG*** is easier and it is more resistant mechanically when using bulk materials.



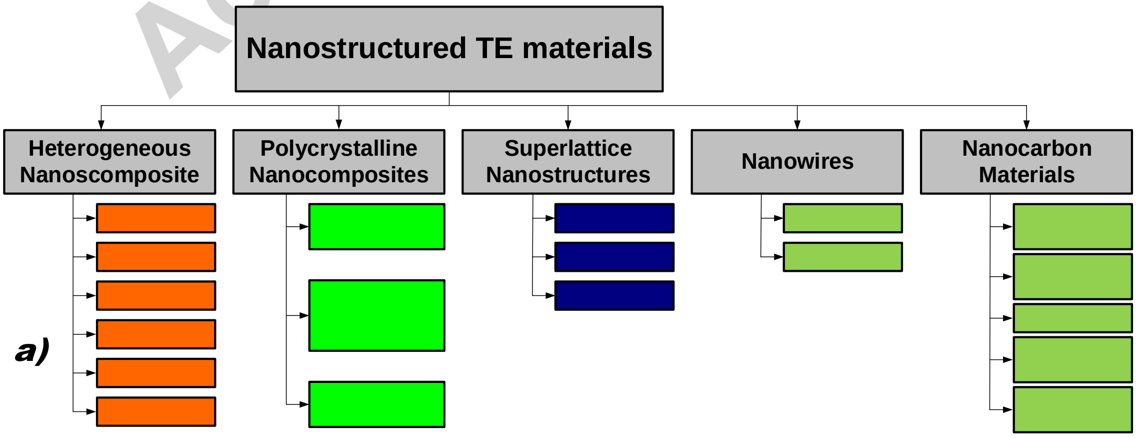

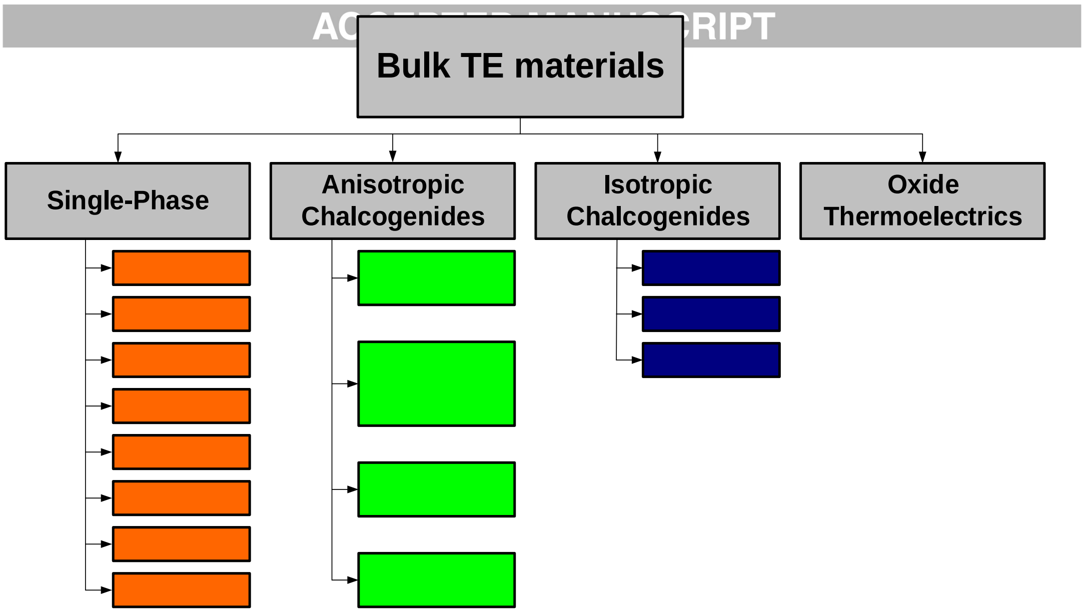


*Fig. 13 Strategies of improving material's zT with a few most common examples* ***a)*** *optimization of zT based on nanostructuration;* ***b)*** *construction of new bulk materials with high zT.*

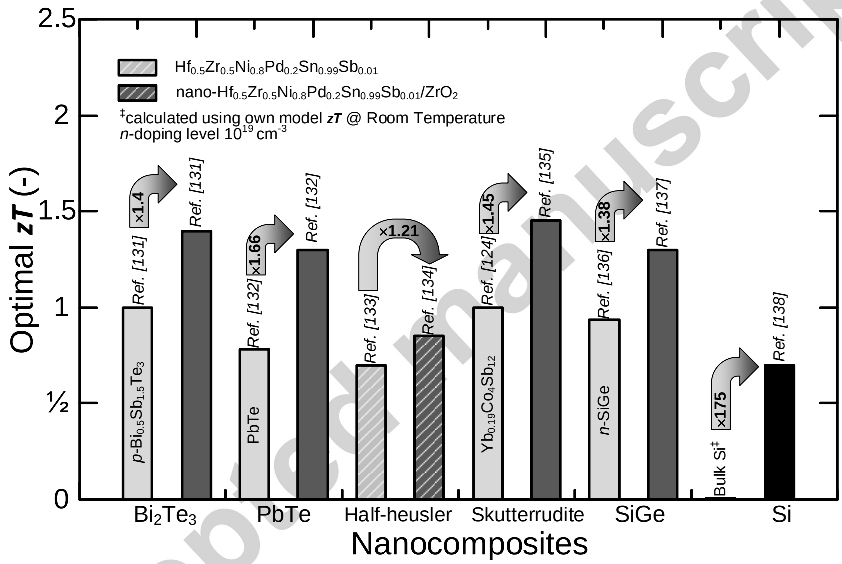


*Fig. 14 Nanostructurally-induced zT improvement of chosen materials; zT values from:* $Bi_2Te_3$ *- [131]; PbTe - [132]; Half-Heusler - [133,134]; Skutterrudite - [124,135]; SiGe - [136,137]; Si - [138].*



Dual efforts on topological (*see Fig. 10*) and material level are significantly contributing to a delivery of increasingly attractive ***TE***s. Fig. 15a graphically presents the improvement history of thermoelectric materials. Although Fig. 15a presents only a fraction of thermoelectric materials reported in the literature, an astonishing increase of interest in thermoelectricity is visible. Owing to a remarkable progress in nanotechnology and material synthesis, thermoelectricity marks outstanding progress aimed towards discovery or construction of high-***zT*** material [139]. According to [140], "*Holy Grail*" for thermoelectricity are bulk materials (both ***n***- and ***p***-type) with low leakages (*low contact resistances, heat radiation*), exhibiting ***zT***≈2-3 (or $\eta_{TE}$=15-20%) and low manufacturing costs. Fig. 15 illustrates that nowadays only few materials are exhibiting ***zT***>2 (*n*-$Bi_2Te_3/Sb_2Te_3$ [141], LAST-18 [142], *p*-SnSe [125] and *n*-SnSe with 2%Bi [143]), but their complex structure, toxicity or sophisticated immature fabrication technology hinders their commercialization. Another issue is a lack of high-***zT*** ***p***- and ***n***-type materials being technologically compatible. While many high-***zT*** materials were reported, most do not have an opposite conduction counterpart or the counterpart's ***zT*** is several times lower. This makes a technological construction of ***TEG*** more difficult (*Fig. 10*), since both ***p***- and ***n***-type materials are needed.

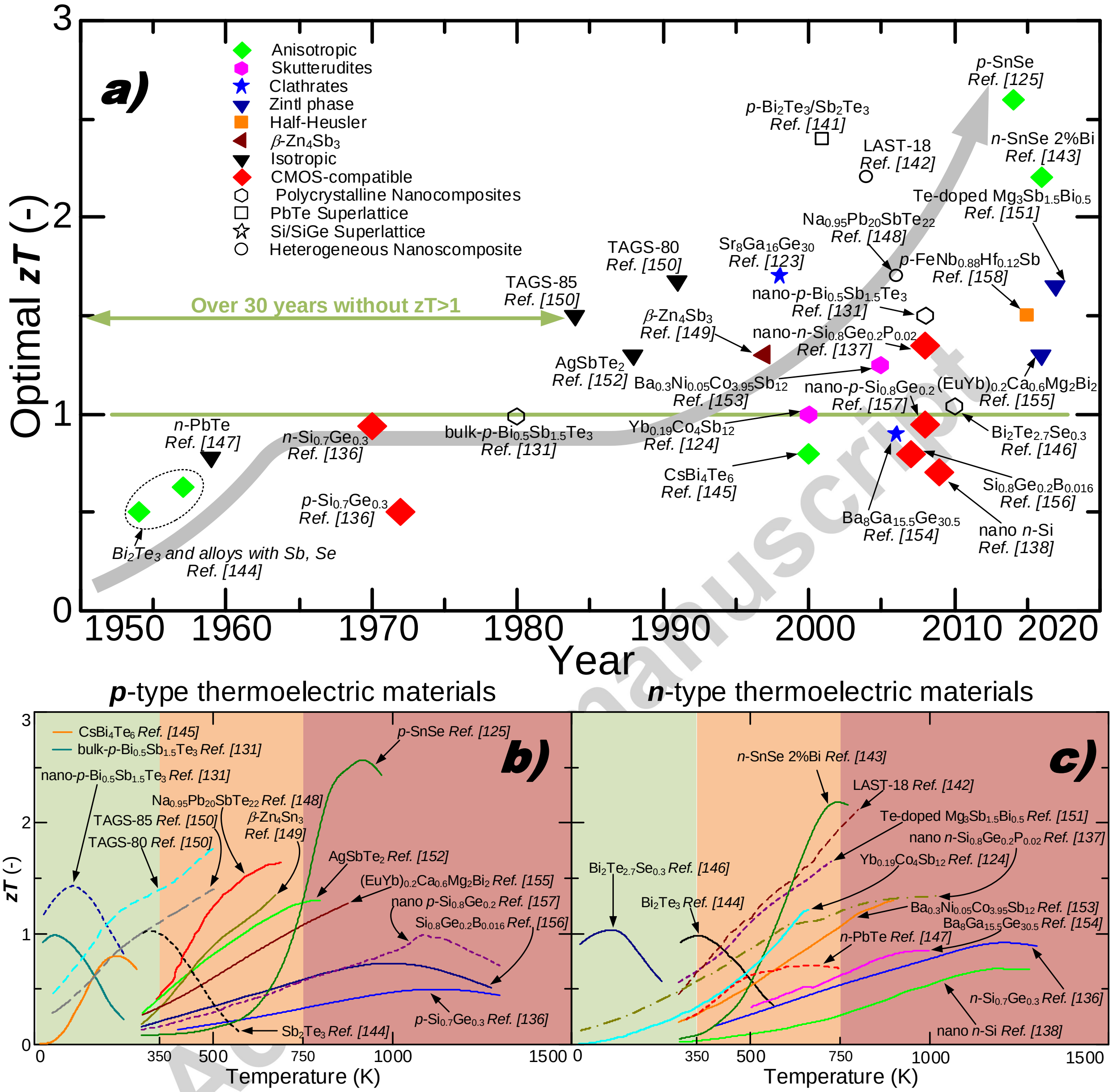


*Fig. 15* ***a)*** *Gradual improvement of thermoelectric non-dimensional-figure-of-merit;* ***b)*** *non-dimensional-figure-of-merit against temperature for typical* ***b)*** *p-type and* ***c)*** *n-type materials data retrieved from:* ***Low range temperature materials*** $\leq$***350K:*** *$Bi_2Te_3$ and $Sb_2Te_3$- [144]; bulk- and nano-p-$Bi_{0.5}Sb_{1.5}Te_3$ - [131]; $CsBi_4Te_6$ - [145]; $Bi_2Te_{2.7}Se_{0.3}$ - [146].* ***Medium range temperature materials*** ***T∈(350K;750K>****: n-PbTe - [147]; p-$Bi_2Te_3/Sb_2Te_3$ - [141]; $Na_{0.95}Pb_{20}SbTe_{22}$ - [148]; $Yb_{0.21}Co_4Sb_{12}$ - [124]; β-$Zn_4Sb_3$ - [149]; TAGS-85 and TAGS-80- [150]; Te-doped $Mg_3Sb_{1.5}Bi_{0.5}$ - [151];* ***High range temperature materials T>750K****: n- and p-SiGe [136]; $AgSbTe_2$ - [152]; p-SnSe - [125]; $Ba_{0.3}Ni_{0.05}Co_{3.95}Sb_{12}$ - [153]; $Ba_8Ga_{15.5}Ge_{30.5}$ - [154]; $Sr_8Ga_{16}Ge_{30}$ - [123]; n-SnSe 2%Bi - [143]; LAST-18 - [142]; nano n-Si [138]; $(EuYb)_{0.2}Ca_{0.6}Mg_2Bi_2$ - [155]; $Si_{0.8}Ge_{0.2}B_{0.016}$ - [156]; nano-p-$Si_{0.8}Ge_{0.2}$ - [157]; nano-n-$Si_{0.8}Ge_{0.2}P_{0.02}$ - [137]; p-$FeNb_{0.88}Hf_{0.12}Sb$ - [158];*

Referring to Eq. 1 ***zT*** depends on three material properties ***σ***, ***κ*** and ***S*** thus making ***zT*** multi-interdependent. Additionally thermopower, thermal and electrical conductivities are dependent on doping concentration and on temperature. Owing to that, different materials exhibits maximal ***zT*** value for different temperatures which is illustrated in Fig. 15b and c. Design of ***TEG*** requires conscious selection of material for precisely identified thermal conditions previewed for ***TEG***. Subsequently optimal doping concentration, for a given material, has to be identified in order to maximize ***zT***.

While the continuous battle to rise ***zT*** puts ***TE*** among one of the most promising and expanding branches of ***EH***, ***TE*** still struggles to gain popularity on the market. Fig. 16a shows historical progress in ***TEG***s power density, and Fig. 16b highlights commercially available ***TEG***s.

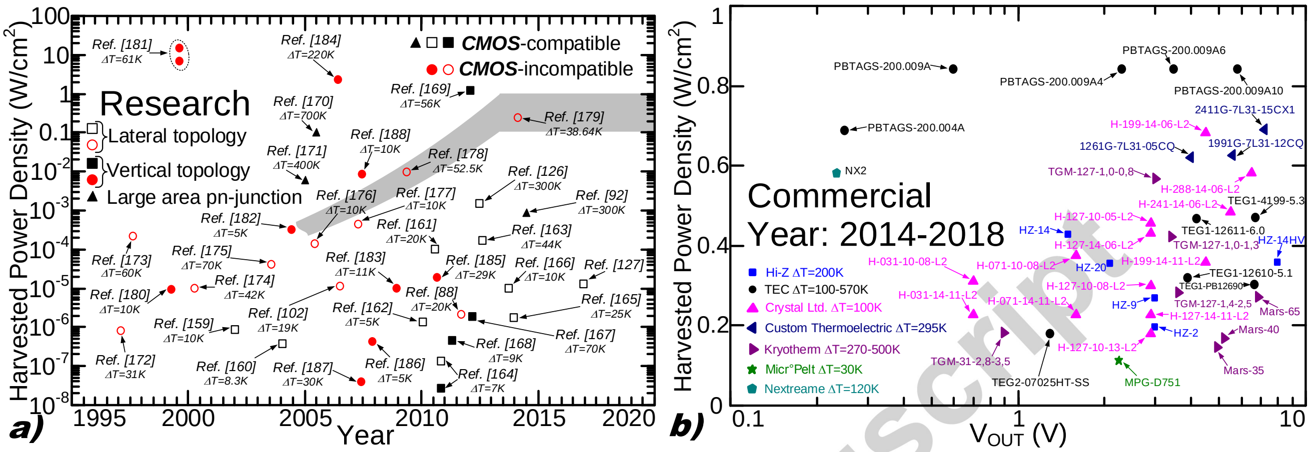


*Fig. 16* ***a)*** *History of optimal harvested power density in research TEGs emphasizing compatibility with CMOS and temperature drop across TEG.* □○ *are for lateral* ■● *are for π-type and* ▲ *for large area pn junction TEG structures:* ***CMOS-compatible generators:*** *lateral (*□*)- [159–163,126,164–166,127], vertical (*■*)- [164,167–169] and large area pn junction (*▲*)- [92,170,171] topology.* ***Incompatible with CMOS:*** *lateral (*○*)- [88,102,172–179] and vertical (*●*)- [180–188] topology.* ***b)*** *Optimal power density versus output voltage for commercialized TEGs from several manufacturers;*

For ***TEG***s in Fig. 16b, an average cost of ~54$/W was calculated which remains unattractive confronted with the average cost for ***PV*** being ~3.5$/W***.*** ***TEG*** price is dominated by the material and its processing. Fig. 15 shows that modern ***TE*** uses materials which are harmful, toxic, complex and thus expensive. ***TE*** "*foundation stone*" materials are compounds of Bismuth (***Bi*** ~10.5$/kg), Tellurium (***Te*** ~36$/kg), Antimony (***Sb*** ~9$/kg), Selenium (***Se*** ~24$/kg) or Lead (***Pb*** ~2.50$/kg) [144,189,190] (*material's cost based on* [191]). On the other hand ***PV*** cost attractiveness lies in cheap fabrication technology based on Silicon (***Si*** ~1.5$/kg). ***TE*** can follow ***PV*** in the cost suppression using ***CMOS***-compatible materials namely ***Si***, Germanium (***Ge***) and Silicon-Germanium ($Si_xGe_{1-x}$). However, ***TE*** requires materials integrating crystal-like electrical and glass-like thermal transports. As a foundations of digital industry, ***CMOS*** materials have very good and well reported electrical properties. Focusing only on electric properties, ***CMOS***-compatible materials can deliver comparable power with conventional $Bi_2Te_3/Sb_2Te_3$ ***TEG***s [85]. Excluding $Si_xGe_{1-x}$, the usage of ***Si*** or ***Ge*** in ***TE*** is problematic due to an excessive bulk thermal conductivity ($\kappa=\kappa_{el}+\kappa_{ph}$) which is dramatically lowering their ***zT*** (*see Eq. 1*). By the means of modern nanotechnology (*thin-film and phononic crystals*) it is now possible to nanostructurally decrease $\kappa$ by suppression of $\kappa_{ph}$ in ***Si***

[192–201] with minor impact on ***σ*** and ***S***. Experimentally confirmed ***κ*** reduction will attractively rise $\eta_{TE}$ (*see Eq. 2*) of ***Si***-based ***TEG***s. For 10nm thick ***Si***-membrane a ×10 efficiency improvement compared with bulk ***Si*** was reported [202]. This inspires scientists to develop ***CMOS***-compatible ***TEG***s, which is visible in rising number of ***CMOS***-compatible materials (*see Fig. 15*) and generators (*see Fig. 16a*). Switching to ***CMOS***-materials and technology can play the same market-launching role as it did for ***PV***, however, further improvement of ***zT*** is still needed.

# 6. SUBJUGATE THERMOELECTRIC ENERGY

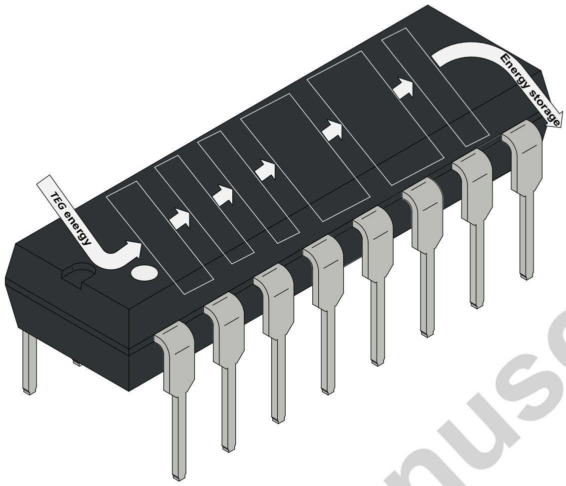


*Fig. 17 Block diagram showing the controlling circuit component blocks*

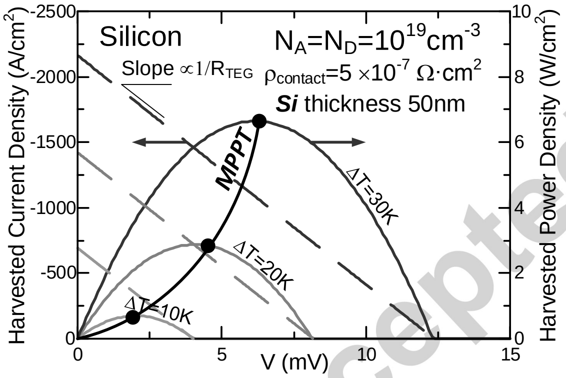


*Fig. 18 Current and power densities versus output voltage for TEG topology depicted in Fig. 10c when using heavily doped 50nm thick Silicon membranes [203]*

Effective power extraction from ***TEG*** requires a use of electronic controllers enabling *i.a.* voltage adaptation, energy storage and ***M***aximal ***P***ower ***P***oint ***T***racking (***MPPT***) [204–206], all this functions are integrated in miniaturized microelectronics package as depicted in Fig. 17. In the most usual case, ***TEG*** operates under imposed thermal conditions and temperature difference across the ***TEG.*** This results in a voltage formation according to the physics of the Seebeck effect (*see Fig. 10b*). Connecting ***TEG*** with variable load resistance ($R_{LOAD}$) allows tracing its output characteristics depicted in the Fig. 18. It is important to note that ***TEG*** is a ***DC*** source as the current-voltage characteristics are linear. Thus, slope of the ***IV*** characteristics depends on the total internal ***TEG*** resistance ($R_{TEG}$). Referring to ***TEG*** harvested power, its maximum ($P_{MAX}$) is achieved for impedance matching condition when $\boldsymbol{R_{TEG}}$=$\boldsymbol{R_{LOAD}}$ [79,165,207–210]. For a given $\boldsymbol{\Delta T}$ and thermopowers ($S_P$,$S_N$) $\boldsymbol{P_{MAX}}$ is defined by Eq. 4 [211–213]:

$$P_{MAX} = \frac{(S_P - S_N)^2 \cdot \Delta T^2}{4 \cdot R_{TEG}} \qquad \textit{Eq. 4}$$

$\boldsymbol{R_{TEG}}$ depends on the temperature, thus for each $\boldsymbol{\Delta T}$ the $\boldsymbol{P_{MAX}}$ is achieved for different $\boldsymbol{R_{LOAD}}$. In practice, ***TEG*** provides energy for a given device, which requires nominal power to operate properly. To ensure continuous alimentation in case of $\boldsymbol{\Delta T}$ short-time decay an energy storage unit (*capacitor or battery*) is inserted between ***TEG*** and the load. In this configuration however, an undesirable situation can occur. When ***TEG*** output voltage is smaller than storage unit voltage, an energy flow from storage unit towards ***TEG*** is observed. To prevent this, at least a blocking diode is necessary. However, diode application in this case is not the smartest solution due to relatively high conduction losses and considerable diode's forward voltage drop lowering ***TEG*** output voltage. Modern power electronics elaborated techniques allowing for ***MPPT*** tracking and providing a fantastic reduction of losses owing to *e.g.* soft switching techniques [214,215]. Electronic circuits sandwiched between ***TEG*** and storage unit are usually named controllers. Their role in a harvesting system is to always maximize extracted power with changing ***TEG***'s thermal conditions, ensuring the shortest charging time for the storage unit and boosting/adapting the ***TEG*** output voltage to the standard operational level. Moreover, controllers are preventing the undesirable inverse energy flow from storage unit towards ***TEG*** in case of $\boldsymbol{\Delta T}$ atrophy.

This is particularly important, since thermoelectricity exhibits rather poor conversion efficiencies (*see Fig. 11*) and any additional losses in the harvesting system are highly undesirable.

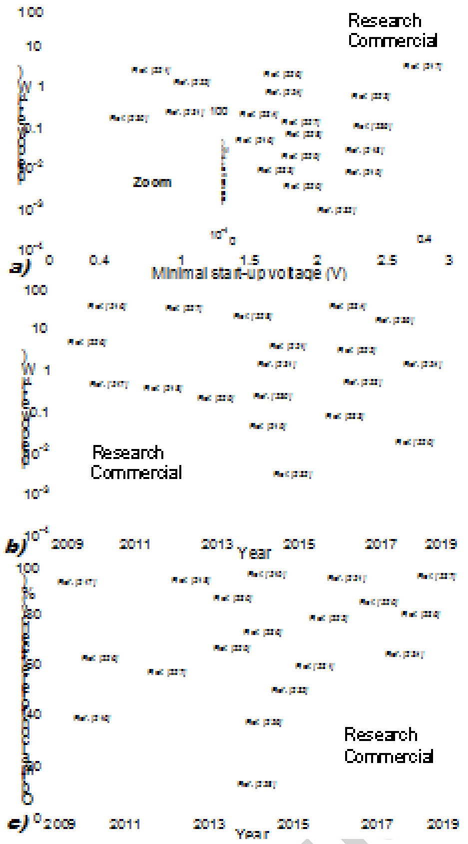


Fig. 19 Review on energy controllers circuits emphasizing **a)** Power consumption in idle mode versus minimal start-up voltage; **b)** historical improvement of rest-state power consumption and **c)** Historical evolution of controllers conversion efficiency. Based on: **Commercial**: [216–225]; **Research**: [226–237]

Fig. 19 summarizes lab-made and commercially available controllers dedicated to ***TE*** harvesting. Considering that ***TEG***s efficiencies are low (*see Fig. 11*), especially around room temperature, a lot of effort is focused on reducing the activation voltage while maintaining the highest possible controller efficiency. Fig. 19a presents idle power consumption versus minimal start-up voltage and reveals that many of controllers for ***TE*** harvesting have start-up voltage way below 100mV. This enables ***TEG*** to extract energy even for very low $\Delta T$, when the output voltage is very small. If the storage unit is to be charged efficiently and quickly, all intermediary devices should consume as little power as possible. Fig. 19b illustrates reduction of idle power over past years and shows that controllers are consuming less and less power which is vital to extend a duration of proper system operation through periods of ***TEG*** insufficiency. Finally, Fig. 19c historically compares optimal controller efficiencies, showing that controllers cooperating with ***TEG***s are becoming more and more efficient. For both research and commercial solutions there are examples of efficiency above 90%.

Fig. 19a, b and c collectively show that low start-up voltage, low idle power and high efficiency are difficult to achieve simultaneously. Wide offer of ***TEG*** controllers allows selection of the most suitable device depending on efficiency, start-up voltage or idle power importance.

# 7. MARKET PERSPECTIVES

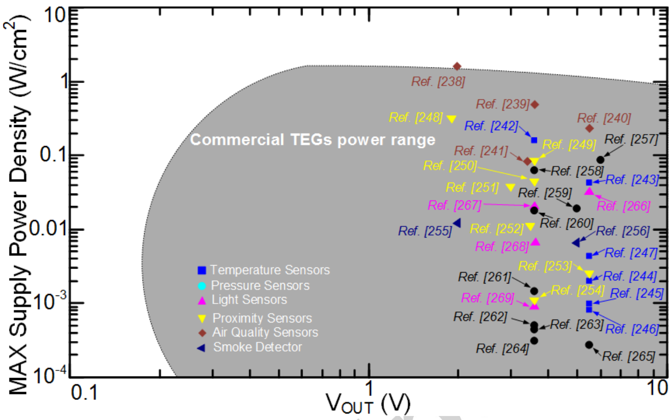


*Fig. 20 Confrontation of maximal supply power density of commercially available IoT sensors [238–269] with TEG power density retrieved from Fig. 16b*

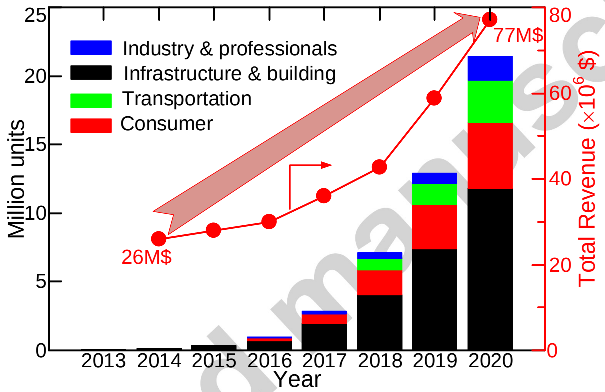


*Fig. 21 Micro-power thermoelectric generator market growth forecast, columns quantify TEG units in use [270] and red line total TEG market revenue [271]*

Already commercially available ***TEG***s (*retrieved from Fig. 16b*) can successfully cover total power needed for sensors that can work in ***IoT***, which is graphically illustrated in Fig. 20. Confronting sensor and commercial ***TEG***s power densities related to their footprint leads to a conclusion that ***TEG***s are able to provide sufficient, convenient, reliable ***DC***-power for ***IoT*** devices of various type. Numerous applications of ***TEG***s in ***IoT*** are currently in study, and the first realizations are commercially available *e.g.* air temperature controllers/regulators [272–274]. ***TEG***s have the most established position as a power supply in automotive industry [275–277], harsh industrial environment [17] and medical care [78,79,177,278,279]. Future of thermoelectric generators will expand ***TEG***s over different applications resulting in large number of units in use (*see Fig. 21*). Market of thermoelectric generators is predicted to grow astonishingly fast, ***C***ompound ***A***nnual ***G***rowth ***R***ate (***CAGR***) is 14.4% over 2016 to 2022 [280] considering micro- and macro-***TEG***s. Focusing on sub-watt ***TEG***s, the market growth is even bigger producing ***CAGR*** as high as 19.8%

from 2014 to 2020 [271] (*see Fig. 21*). The above arguments show that thermoelectricity has almost all cards in hands to conquer the power supply for ***IoT***. Nevertheless, we have to be aware that still more research is needed especially in the field of thermoelectric materials, where the "*Holy Grail"* material with ***zT***>3 is still beyond reach.

Multiple efforts towards material, topological and electronic optimization are continually boosting ***TEG***s performance. Recent years are showing significant research activity acceleration especially in the field of materials and electronic circuits. Thanks to that, ***TE*** is now closer than ever before to pass the popularization threshold and will surely do it as soon as further ***zT*** improvement in cheap and industrially compatible materials is achieved.

# 8. CONCLUSIONS

This review compares and evaluates recent progress in the field of thermoelectricity with the emphasis on possible use in the ***I***nternet ***o***f ***T***hings (***IoT***) devices. ***IoT*** creates and builds a market bigger than ever known before. Despite of the fact that typical ***IoT*** nodes require very small amount of energy to operate, powering them is problematic, regarding their portability, localization, size and often harsh work environment. At present ***IoT*** nodes are usually supplied using batteries or wires, which is expensive, requires periodic human maintenance and pollutes natural environment. Alternative supply using waste energy harvesting can significantly accelerate further expansion of ***IoT***. In this context, the choice of ***T***hermo***E***lectricity (***TE***) is intuitive, taking into account the omnipresence of the source energy (*domestic, industrial, automotive, human, etc.*) and its enormous size due to the magnitude of heat losses. Additionally, the attractiveness of ***TE*** is amplified by a reliable, silent, vibrationless and direct conversion.

Development of thermoelectricity follows two branches: (i) boosting thermoelectric material performance and (ii) topological ***TEG***s improvement. The prior is prevailing and concentrates either on delivering completely new materials or nanostructuring existing ones to rise-up their thermoelectric performance. Both approaches are very fruitful, and have enabled recently considerable improvements in ***zT***. The progress in the thermoelectric materials currently converges towards ***zT*** slightly below 3. Surpassing ***zT***=3 and maintaining low fabrication costs for both *n*-type and *p*-type material is predicted to be a threshold launching ***TE*** popularization on the market. Furthermore, ***TE*** expansion on the market can be achieved also by increasing industrial compatibility and lowering integration costs. Towards this goal, the conventional materials used in digital industry can be adapted for ***TEG***s fabrication. Owing to this approach, significant ***zT*** improvement of ***CMOS***-compatible materials has been achieved. ***zT*** in nanostructured ***CMOS*** materials may still be smaller, but is balanced by industrial compatibility, low cost, availability, simplicity, harmlessness and possibility of full monolithic integration on chip. However, introducing ***CMOS*** compatible ***TEG***s to massive production requires further improvements of ***zT***. Apart from material improvements, ***TE*** progresses also through reshaping generator's topologies. In response to the industry demands, lateral and large area *pn*-junction ***TEG*** topologies were proposed. Their advantages relies mainly on the ease of large-scale and cheap production and better topological adaptation with already industrially fabricated devices.

Even the best ***TEG*** alone cannot be effectively and efficiently used in ***IoT*** systems. It requires additional circuitry providing *i.a.* maximal power extraction for given thermal conditions, energy autonomy when ***TEG*** energy is insufficient, voltage adaptation *etc*. Those tasks are performed by electronic controllers dedicated to work with ***TEG***s. In this field ***TE*** revealed also outstanding progress both on research and commercial solutions. Modern controllers are able to start-up from ultralow input voltage as small as 20mV, consume extremely low quiescent power around 0.1μW or achieve above 90% conversion efficiency. Merging abovementioned parameters in one device will be a huge achievement significantly contributing to ***TEG*** popularization.



References


[1] REN21, Renewables 2018: Global Status Report, Renewable Energy Policy Network for the 21st Century (REN21), Paris, France, 2018. http://www.ren21.net/wp-content/uploads/2018/06/17-8652_GSR2018_FullReport_web_-1.pdf (accessed September 20, 2018).

[2] British Petroleum, 67th Statistical review of World Energy June 2018, British Petroleum, 2018. https://www.bp.com/content/dam/bp/en/corporate/pdf/energy-economics/statistical-review/bp-stats-review-2018-full-report.pdf (accessed September 20, 2018).

[3] J. Laherrère, Uncertainty of data and forecasts for fossil fuels, Association for the Study of Peak Oil, Universidad de Castilla - La Mancha, 2007. http://www.hubbertpeak.com/laherrere/Castilla200704.pdf (accessed September 20, 2018).

[4] J. Schindler, W. Zittel, Coal: Resources and future production, Energy Watch Group, Berlin, 2007. https://www.energiestiftung.ch/files/energiestiftung/publikationen/downloads/energiethemen-fossileenergien-kohle/ewg_report_coal_10-07-2007ms.pdf (accessed September 20, 2018).

[5] L. de Sousa, World oil and gas production forecasts up to 2100, The Oil Drum. (2013). http://europe.theoildrum.com/node/3565 (accessed September 20, 2018).

[6] F.H. Cocks, Energy demand and climate change: issues and resolutions, Wiley-VCH, Weinheim, 2009.

[7] M.G. Flanner, Integrating anthropogenic heat flux with global climate models, Geophys. Res. Lett. 36 (2009) L02801. doi:10.1029/2008GL036465.

[8] NASA Global Climate, Carbon Dioxide, Climate Change: Vital Signs of the Planet. (2018). https://climate.nasa.gov/vital-signs/carbon-dioxide/ (accessed September 20, 2018).

[9] NASA Global Climate, Global surface temperature, Climate Change: Vital Signs of the Planet. (2018). https://climate.nasa.gov/vital-signs/global-temperature (accessed September 20, 2018).

[10] J. Benes, M. Chauvet, O. Kamenik, M. Kumhof, D. Laxton, S. Mursula, J. Selody, The future of oil: Geology versus technology, Int. J. Forecast. 31 (2015) 207–221. doi:10.1016/j.ijforecast.2014.03.012.

[11] I. Dincer, C. Zamfirescu, Advanced Power Generation Systems, Academic Press, 2014.

[12] Cisco, Internet of Everything (IoE) Connections Counter, (2013). https://newsroom.cisco.com/feature-content?articleId=1208342.

[13] S. Konomi, G. Roussos, eds., Enriching urban spaces with ambient computing, the internet of things, and smart city design, Engineering Science Reference, an imprint of IGI Global, Hershey, PA, 2017.

[14] M. Chen, S. Gonzalez, A. Vasilakos, H. Cao, V.C.M. Leung, Body area networks: A survey, Mobile Networks and Applications. 16 (2011) 171–193. doi:10.1007/s11036-010-0260-8.

[15] B. Latré, B. Braem, I. Moerman, C. Blondia, P. Demeester, A survey on wireless body area networks, Wireless Networks. 17 (2011) 1–18. doi:10.1007/s11276-010-0252-4.

[16] P. Szulewski, Industrial automation products in the conception of Industry 4.0, Mechanik. (2016) 926–933. doi:10.17814/mechanik.2016.8-9.329.

[17] P. Nenninger, U. Marco, Harvest time, ABB Review. 1 (2011) 47–51.

[18] A. Al-Fuqaha, M. Guizani, M. Mohammadi, M. Aledhari, M. Ayyash, Internet of Things: A Survey on Enabling Technologies, Protocols, and Applications, IEEE Communications Surveys Tutorials. 17 (2015) 2347–2376. doi:10.1109/COMST.2015.2444095.

[19] S. Mclelland, Intelligent buildings: sensing a need?, Sensor Review. 8 (1988) 128–130. doi:10.1108/eb007763.

[20] C. Perera, Sensing as a Service for Internet of Things: A Roadmap, 2017.

[21] C.X. Mavromoustakis, G. Mastorakis, J.M. Batalla, Internet of Things (IoT) in 5G Mobile Technologies, 2016. http://dx.doi.org/10.1007/978-3-319-30913-2 (accessed March 9, 2018).

[22] Q.F. Hassan, A. ur R. Khan, S.A. Madani, Internet of Things: Challenges, Advances, and Applications, CRC Press, 2017.

[21] T. Skotnicki, “Energy harvesting for IoT”, short course at the 2015 Symposia on VLSI Technology and Circuits, Kyoto, Japan, 15-Jun-2015.

[24] N. Elvin, A. Erturk, Advances in Energy Harvesting Methods, Springer, New York, NY, 2013.

[25] D. Briand, E. Yeatman, S. Roundy, eds., Micro energy harvesting, 1<sup>st</sup> edition, Wiley-VCH, Weinheim, 2015.

[26] L.B. Kong, T. Li, H.H. Hng, F. Boey, T. Zhang, S. Li, Waste energy harvesting, Springer Berlin Heidelberg, Berlin, Heidelberg, 2014. http://link.springer.com/10.1007/978-3-642-54634-1 (accessed April 21, 2014).

[27] T.K. Ghosh, M.A. Prelas, T.K. Ghosh, Renewable Resources, Springer, Dordrecht, 2011.

[28] I. Staffell, D.J.L. Brett, N.P. Brandon, A.D. Hawkes, eds., Domestic microgeneration: renewable and distributed energy technologies, policies, and economics, Routledge, New York, 2015.

[29] T. Suntio, T. Messo, J. Puukko, Wiley-VCH, Power Electronic Converters Dynamics and Control in Conventional and Renewable Energy Applications, Wiley-VCH Verlag GmbH & Co. KGaA, Boschstr. 12, 69469 Weinheim, Germany, 2018.

[30] M.Z. Jacobson, M.A. Delucchi, Providing all global energy with wind, water, and solar power, Part I: Technologies, energy resources, quantities and areas of infrastructure, and materials, Energy Policy. 39 (2011) 1154–1169. doi:10.1016/j.enpol.2010.11.040.

[31] R.J.M. Vullers, R. van Schaijk, I. Doms, C. Van Hoof, R. Mertens, Micropower energy harvesting, Solid-State Electronics. 53 (2009) 684–693. doi:10.1016/j.sse.2008.12.011.

[32] J.W. Matiko, N.J. Grabham, S.P. Beeby, M.J. Tudor, Review of the application of energy harvesting in buildings, Meas. Sci. Technol. 25 (2014) 012002. doi:10.1088/0957-0233/25/1/012002.

[33] H.J. Visser, A.C.F. Reniers, J.A.C. Theeuwes, Ambient RF Energy Scavenging: GSM and WLAN Power Density Measurements, in: 38Th European Microwave Conference EuMC 2008, 2008: pp. 721–724. doi:10.1109/EUMC.2008.4751554.

[34] S. Duangsuwan, T. Leukachorn, S. Chinsawatpan, S. Promwong, Experimental study for polarimetric measurement of RFID transfer function with in an indoor environment, in: 2009 IEEE 9Th Malaysia International Conference on Communications (MICC), 2009: pp. 686–690. doi:10.1109/MICC.2009.5431410.

[35] S. Sherrit, H.J. Lee, P. Walkemeyer, T. Winn, L.P. Tosi, T. Colonius, Fluid flow nozzle energy harvesters, in: Sensors and Smart Structures Technologies for Civil, Mechanical, and Aerospace Systems 2015, International Society for Optics and Photonics, 2015: p. 943507. doi:10.1117/12.2084574.

[36] H. Lee, S. Sherrit, L. Tosi, P. Walkemeyer, T. Colonius, Piezoelectric Energy Harvesting in Internal Fluid Flow, Sensors. 15 (2015) 26039–26062. doi:10.3390/s151026039.

[37] IEC 61215-1:2016, Terrestrial photovoltaic (PV) modules - Design qualification and type approval - Part 1: Test requirements, International Electrotechnical Commission (IEC), 2016. https://webstore.iec.ch/publication/24312’.

[38] D.A. Howey, A. Bansal, A.S. Holmes, Design and performance of a centimetre-scale shrouded wind turbine for energy harvesting, Smart Mater. Struct. 20 (2011) 085021. doi:10.1088/0964-1726/20/8/085021.

[39] A.S. Holmes, G. Hong, K.R. Pullen, K.R. Buffard, Axial-flow microturbine with electromagnetic generator: design, CFD simulation, and prototype demonstration, in: 17Th IEEE International Conference on Micro Electro Mechanical Systems, 2004 (MEMS), 2004: pp. 568–571. doi:10.1109/MEMS.2004.1290648.

[40] ANSI/ASHRAE/IES Standard 90.1-2016, Energy Standard for Buildings Except Low-Rise Residential Buildings, 2016.

[41] S. Roundy, P.K. Wright, J.M. Rabaey, Energy Scavenging for Wireless Sensor Networks with Special Focus on Vibrations, Springer US, Boston, MA, 2004.

[42] United Nations, Department of Economic and Social Affairs, Population Division, World population prospects, United Nations, 2015. https://esa.un.org/unpd/wpp/Download/Standard/Population/.

[43] T. Starner, J.A. Paradiso, Human Generated Power for Mobile Electronics, in: Low-Power Electronics Design, Boca Raton, 2004: pp. 1–35.

[44] R. Caliò, U. Rongala, D. Camboni, M. Milazzo, C. Stefanini, G. de Petris, C. Oddo, Piezoelectric Energy Harvesting Solutions, Sensors. 14 (2014) 4755–4790. doi:10.3390/s140304755.

[45] D.-S. Kwon, H.-J. Ko, J. Kim, Piezoelectric and electromagnetic hybrid energy harvester using two cantilevers for frequency up-conversion, in: IEEE, 2017: pp. 49–52. doi:10.1109/MEMSYS.2017.7863336.

[46] P. Li, S. Gao, B. Cong, Theoretical modeling, simulation and experimental study of hybrid piezoelectric and electromagnetic energy harvester, AIP Advances. 8 (2018) 035017. doi:10.1063/1.5018836.

[47] K. Fan, S. Liu, H. Liu, Y. Zhu, W. Wang, D. Zhang, Scavenging energy from ultra-low frequency mechanical excitations through a bi-directional hybrid energy harvester, Applied Energy. 216 (2018) 8–20. doi:10.1016/j.apenergy.2018.02.086.

[48] V.R. Challa, M.G. Prasad, F.T. Fisher, A coupled piezoelectric–electromagnetic energy harvesting technique for achieving increased power output through damping matching, Smart Mater. Struct. 18 (2009) 095029. doi:10.1088/0964-1726/18/9/095029.

[49] Z. Xu, X. Shan, D. Chen, T. Xie, A Novel Tunable Multi-Frequency Hybrid Vibration Energy Harvester Using Piezoelectric and Electromagnetic Conversion Mechanisms, Applied Sciences. 6 (2016) 10. doi:10.3390/app6010010.

[50] L. Jin, J. Chen, B. Zhang, W. Deng, L. Zhang, H. Zhang, X. Huang, M. Zhu, W. Yang, Z.L. Wang, Self-Powered Safety Helmet Based on Hybridized Nanogenerator for Emergency, ACS Nano. 10 (2016) 7874–7881. doi:10.1021/acsnano.6b03760.

[51] R.K. Gupta, Q. Shi, L. Dhakar, T. Wang, C.H. Heng, C. Lee, Broadband Energy Harvester Using Non-linear Polymer Spring and Electromagnetic/Triboelectric Hybrid Mechanism, Scientific Reports. 7 (2017) 41396. doi:10.1038/srep41396.

[52] B. Zhang, J. Chen, L. Jin, W. Deng, L. Zhang, H. Zhang, M. Zhu, W. Yang, Z.L. Wang, Rotating-Disk-Based Hybridized Electromagnetic–Triboelectric Nanogenerator for Sustainably Powering Wireless Traffic Volume Sensors, ACS Nano. 10 (2016) 6241–6247. doi:10.1021/acsnano.6b02384.

[53] M. Salauddin, R.M. Toyabur, P. Maharjan, J.Y. Park, High performance human-induced vibration driven hybrid energy harvester for powering portable electronics, Nano Energy. 45 (2018) 236–246. doi:10.1016/j.nanoen.2017.12.046.

[54] M. Salauddin, H. Cho, J.Y. Park, A Hybrid Electromagnetic-Triboelectric Energy Harvester Using a Dual Halbach Magnet Array Powered by Human-Body-Induced Motion, Advanced Materials Technologies. 3 (2018) 1700240. doi:10.1002/admt.201700240.

[55] J. Zhu, Y. Zhu, X. Wang, A Hybrid Piezoelectric and Triboelectric Nanogenerator with PVDF Nanoparticles and Leaf-Shaped Microstructure PTFE Film for Scavenging Mechanical Energy, Advanced Materials Interfaces. 5 (2018) 1700750. doi:10.1002/admi.201700750.

[56] Y. Yang, Z.L. Wang, Hybrid energy cells for simultaneously harvesting multi-types of energies, Nano Energy. 14 (2015) 245–256. doi:10.1016/j.nanoen.2014.11.058.

[57] K. Zhang, S. Wang, Y. Yang, A One-Structure-Based Piezo-Tribo-Pyro-Photoelectric Effects Coupled Nanogenerator for Simultaneously Scavenging Mechanical, Thermal, and Solar Energies, Adv. Energy Mater. 7 (2017) 1601852. doi:10.1002/aenm.201601852.

[58] Y. Yang, H. Zhang, G. Zhu, S. Lee, Z.-H. Lin, Z.L. Wang, Flexible Hybrid Energy Cell for Simultaneously Harvesting Thermal, Mechanical, and Solar Energies, ACS Nano. 7 (2013) 785–790. doi:10.1021/nn305247x.

[59] X. Wang, Z.L. Wang, Y. Yang, Hybridized nanogenerator for simultaneously scavenging mechanical and thermal energies by electromagnetic-triboelectric-thermoelectric effects, Nano Energy. 26 (2016) 164–171. doi:10.1016/j.nanoen.2016.05.032.

[60] Y. Wu, X. Zhong, X. Wang, Y. Yang, Z.L. Wang, Hybrid energy cell for simultaneously harvesting wind, solar, and chemical energies, Nano Res. 7 (2014) 1631–1639. doi:10.1007/s12274-014-0523-y.

[61] K. Zhang, Y. Yang, Thermo-Phototronic Effect Enhanced InP/ZnO Nanorod Heterojunction Solar Cells for Self-Powered Wearable Electronics, Adv. Funct. Mater. 27 (2017) 1703331. doi:10.1002/adfm.201703331.

[62] S. Wang, Z.L. Wang, Y. Yang, A One-Structure-Based Hybridized Nanogenerator for Scavenging Mechanical and Thermal Energies by Triboelectric–Piezoelectric–Pyroelectric Effects, Adv. Mater. 28 (2016) 2881–2887. doi:10.1002/adma.201505684.

[63] N. Bizon, N.M. Tabatabaei, F. Blaabjerg, E. Kurt, eds., Energy Harvesting and Energy Efficiency: Technology, Methods, and Applications, Springer International Publishing, 2017.

[64] R. Allan, Energy harvesting efforts are picking up steam, Power Electronics. (2012). http://www.powerelectronics.com/energy-harvesting/energy-harvesting-efforts-are-picking-steam (accessed November 14, 2017).

[65] P. Harrop, R. Das, Energy harvesting and storage for electronic devices 2009-2019, IDTechEx Ltd., Cambridge, CB25 0NW United Kingdom, 2009.

[66] M. Raju, M. Grazier, Energy Harvesting ULP meets energy harvesting: A game-changing combination for design engineers., (2010). http://www.ti.com/lit/wp/slyy018a/slyy018a.pdf?DCMP=tmg-issccpr-021712&HQS=issccpr-wp.

[67] B. Priyantha, D. Lymberopoulos, J. Liu, EERS: Energy Efficient Responsive Sleeping on Mobile Phones, Microsoft Research. (n.d.) 2010.

[68] E.L. Cook, The flow of energy in an industrial society, Sci. Am. 225 (1971) 135–142. doi:10.1038/scientificamerican0971-134.

[69] Energetics, Energy use loss and opportunities analysis: U.S. manufacturing & mining, US Department of Energy, 2004.

[70] Y. Yang, Y. Zhou, J.M. Wu, Z.L. Wang, Single Micro/Nanowire Pyroelectric Nanogenerators as Self-Powered Temperature Sensors, ACS Nano. 6 (2012) 8456–8461. doi:10.1021/nn303414u.

[71] Y. Yang, W. Guo, K.C. Pradel, G. Zhu, Y. Zhou, Y. Zhang, Y. Hu, L. Lin, Z.L. Wang, Pyroelectric Nanogenerators for Harvesting Thermoelectric Energy, Nano Lett. 12 (2012) 2833–2838. doi:10.1021/nl3003039.

[72] Y. Yang, S. Wang, Y. Zhang, Z.L. Wang, Pyroelectric Nanogenerators for Driving Wireless Sensors, Nano Lett. 12 (2012) 6408–6413. doi:10.1021/nl303755m.

[73] E. Velmre, Thomas Johann Seebeck and his contribution to the modern science and technology, in: 12$^{Th}$ Biennial Baltic Electronics Conference (BEC), 2010, 2010: pp. 17–24. doi:10.1109/BEC.2010.5631216.

[74] T.M. Tritt, Thermoelectric phenomena, materials and applications, Annu. Rev. Mater. Res. 41 (2011) 433–448. doi:10.1146/annurev-matsci-062910-100453.

[75] A.K. Misra, Overview of NASA program on development of radioisotope power systems with high specific power, in: San Diego, California, 2006: pp. 1388–1394. http://arc.aiaa.org/doi/abs/10.2514/6.2006-4187.

[76] J. Yang, T. Caillat, Thermoelectric materials for space and automotive power generation, MRS Bull. 31 (2006) 224–229. doi:10.1557/mrs2006.49.

[77] D.M. Rowe, Applications of nuclear-powered thermoelectric generators in space, Applied Energy. 40 (1991) 241–271. doi:10.1016/0306-2619(91)90020-X.

[78] L. Francioso, C. De Pascali, I. Farella, C. Martucci, P. Cretì, P. Siciliano, A. Perrone, Flexible thermoelectric generator for ambient assisted living wearable biometric sensors, J. Power Sources. 196 (2011) 3239–3243. doi:10.1016/j.jpowsour.2010.11.081.

[79] V. Leonov, P. Fiorini, T. Torfs, R.J.M. Vullers, C. Van Hoof, Thermal matching of a thermoelectric energy harvester with the environment and its application in wearable self-powered wireless medical sensors, in: $15^{Th}$ International Workshop on Thermal Investigations of ICs and Systems, THERMINIC 2009, 2009: pp. 95–100.

[80] C. Yu, K.T. Chau, Thermoelectric automotive waste heat energy recovery using maximum power point tracking, Energy Convers. Manage. 50 (2009) 1506–1512. doi:10.1016/j.enconman.2009.02.015.

[81] Z.B. Tang, Y.D. Deng, C.Q. Su, W.W. Shuai, C.J. Xie, A research on thermoelectric generator's electrical performance under temperature mismatch conditions for automotive waste heat recovery system, Case Studies in Thermal Engineering. 5 (2015) 143–150. doi:10.1016/j.csite.2015.03.006.

[82] G. Meisner, Advanced Thermoelectric Materials and Generator Technology for Automotive Waste Heat at GM, (2011). http://www1.eere.energy.gov/vehiclesandfuels/pdfs/thermoelectrics_app_2011/monday/meisner.pdf (accessed February 24, 2015).

[83] D.M. Rowe, C.M. Bhandari, Modern Thermoelectrics, Holt-Technology, 1983.

[84] J. Nurnus, H. Bottner, A. Lambrecht, Thermoelectric micro devices: Interplay of highly effective thin film materials and technological compatibility, in: $22^{Nd}$ International Conference on Thermoelectrics - ICT, 2003, La Grande Motte, France, 2003: pp. 655–660. doi:10.1109/ICT.2003.1287598.

[85] M. Haras, V. Lacatena, S. Monfray, J.-F. Robillard, T. Skotnicki, E. Dubois, Unconventional thin-film thermoelectric converters: structure, simulation, and comparative study, J. Electron. Mater. 43 (2014) 2109–2114. doi:10.1007/s11664-014-2982-z.

[86] J.P. Carmo, L.M. Goncalves, J.H. Correia, Micro and Nanodevices for thermoelectric converters, in: B. Bhushan (Ed.), Scanning Probe Microscopy in Nanoscience and Nanotechnology, Springer, Heidelberg, 2010: pp. 791–811. http://public.eblib.com/EBLPublic/PublicView.do?ptiID=666889 (accessed October 24, 2013).

[87] L.M. Goncalves, J.G. Rocha, C. Couto, P. Alpuim, G. Min, D.M. Rowe, J.H. Correia, Fabrication of flexible thermoelectric microcoolers using planar thin-film technologies, J. Micromech. Microeng. 17 (2007) 168–173. doi:10.1088/0960-1317/17/7/S14.

[88] A. Chen, D. Madan, P.K. Wright, J.W. Evans, Dispenser-printed planar thick-film thermoelectric energy generators, J. Micromech. Microeng. 21 (2011) 104006. doi:10.1088/0960-1317/21/10/104006.

[89] G. Span, M. Wagner, S. Holzer, T. Grasser, Thermoelectric Power Conversion using Generation of Electron-Hole Pairs in Large Area pn Junctions, in: The $25^{Th}$ International Conference on Thermoelectrics, IEEE, Vienna, Austria, 2006: pp. 23–28. doi:10.1109/ICT.2006.331261.

[90] G. Span, M. Wagner, T. Grasser, L. Holmgren, Miniaturized TEG with thermal generation of free carriers, Physica Status Solidi (RRL) – Rapid Research Letters. 1 (2007) 241–243. doi:10.1002/pssr.200701171.

[91] R. Chavez, A. Becker, V. Kessler, M. Engenhorst, N. Petermann, H. Wiggers, G. Schierning, R. Schmechel, A new thermoelectric concept using large area PN junctions, MRS Proceedings. 1543 (2013) 3–8. doi:10.1557/opl.2013.954.

[92] R. Chavez, S. Angst, J. Hall, J. Stoetzel, V. Kessler, L. Bitzer, F. Maculewicz, N. Benson, H. Wiggers, D. Wolf, G. Schierning, R. Schmechel, High Temperature Thermoelectric Device Concept Using Large Area <Emphasis Type="Italic">PN</Emphasis> Junctions, J. Electron. Mater. 43 (2014) 2376–2383. doi:10.1007/s11664-014-3073-x.

[93] M. Wagner, G. Span, S. Holzer, O. Triebl, T. Grasser, V. Palankovski, Power Output Improvement of Silicon-Germanium Thermoelectric Generators, in: Cancun, Mexico, 2006: pp. 1151–1162. doi:10.1149/1.2355909.

[94] R. He, G. Schierning, K. Nielsch, Thermoelectric Devices: A Review of Devices, Architectures, and Contact Optimization, Advanced Materials Technologies. 3 (n.d.) 1700256. doi:10.1002/admt.201700256.

[95] D.M. Rowe, Miniature Semiconductor Thermoelectric Devices, in: CRC Handbook of Thermoelectrics, CRC Press, Boca Raton, FL, 1995: pp. 441–458.

[96] M.A. Korzhuev, L.D. Ivanova, L.I. Petrova, Y.V. Granatkina, T.E. Svechnikova, The Multistage Thermoelectric Devices with Inhomogeneous Legs, in: Proceedings of the $5^{Th}$ European Conference on Thermoelectrics, Odessa, Ukraine, 2007.

[97] G.S. Hwang, A.J. Gross, H. Kim, S.W. Lee, N. Ghafouri, B.L. Huang, C. Lawrence, C. Uher, K. Najafi, M. Kaviany, Micro thermoelectric cooler: Planar multistage, Int. J. Heat Mass Transfer. 52 (2009) 1843–1852. doi:10.1016/j.ijheatmasstransfer.2008.10.014.

[98] B.W. Swanson, E.V. Somers, R.R. Heikes, Optimization of a Sandwiched Thermoelectric Device, J. Heat Transfer. 83 (1961) 77–82. doi:10.1115/1.3680473.

[99] T. Caillat, J.P. Fleurial, G.J. Snyder, A. Borshchevsky, Development of high efficiency segmented thermoelectric unicouples, in: Proceedings of the $20^{Th}$ International Conference on Thermoelectrics (ICT2001), IEEE, Beijing, China, 2001: pp. 282–285. doi:10.1109/ICT.2001.979888.

[100] G.J. Snyder, Application of the compatibility factor to the design of segmented and cascaded thermoelectric generators, Applied Physics Letters. 84 (2004) 2436–2438. doi:doi:10.1063/1.1689396.

[101] D.T. Crane, An Introduction to System-Level, Steady-State and Transient Modeling and Optimization of High-Power-Density Thermoelectric Generator Devices Made of Segmented Thermoelectric Elements, J. Electron. Mater. 40 (2011) 561–569. doi:10.1007/s11664-010-1451-6.

[102] J. Weber, K. Potje-Kamloth, F. Haase, P. Detemple, F. Völklein, T. Doll, Coin-size coiled-up polymer foil thermoelectric power generator for wearable electronics, Sens. Actuators A: Phys. 132 (2006) 325–330. doi:10.1016/j.sna.2006.04.054.

[103] Z. Cao, E. Koukharenko, M.J. Tudor, R.N. Torah, S.P. Beeby, Flexible screen printed thermoelectric generator with enhanced processes and materials, Sens. Actuators A: Phys. 238 (2016) 196–206. doi:10.1016/j.sna.2015.12.016.

[104] M. Hyland, H. Hunter, J. Liu, E. Veety, D. Vashaee, Wearable thermoelectric generators for human body heat harvesting, Appl. Energy. 182 (2016) 518–524. doi:10.1016/j.apenergy.2016.08.150.

[105] F. Suarez, D.P. Parekh, C. Ladd, D. Vashaee, M.D. Dickey, M.C. Öztürk, Flexible thermoelectric generator using bulk legs and liquid metal interconnects for wearable electronics, Appl. Energy. 202 (2017) 736–745. doi:10.1016/j.apenergy.2017.05.181.

[106] R. Alimov, Radioisotope thermoelectric generators, in: Bellona Web. 2011, 2005: p. 21.

[107] D.M. Rowe, Thermoelectric power generation, Proc. IEE. 125 (1978) 1113–1136. doi:10.1049/piee.1978.0247.

[108] G. Min, D.M. Rowe, Conversion efficiency of thermoelectric combustion systems, IEEE Trans. Energy Convers. 22 (2007) 528–534. doi:10.1109/TEC.2006.877375.

[109] C.B. Vining, An inconvenient truth about thermoelectrics, Nat. Mater. 8 (2009) 83–85. doi:10.1038/nmat2361.

[110] S. Volz, ed., Thermal Nanosystems and Nanomaterials, Springer Berlin Heidelberg, Berlin, Heidelberg, 2009. http://link.springer.com/10.1007/978-3-642-04258-4 (accessed March 24, 2015).

[111] A. Shakouri, Recent Developments in Semiconductor Thermoelectric Physics and Materials, Annu. Rev. Mater. Res. 41 (2011) 399–431. doi:10.1146/annurev-matsci-062910-100445.

[112] G.A. Slack, New Materials and performance limits for thermoelectric cooling, in: CRC Handbook of Thermoelectrics, CRC Press, Boca Raton, FL, 1995.

[113] J.M. Ziman, Electrons and phonons: the theory of transport phenomena in solids, Clarendon Press; Oxford University Press, Oxford: New York, 2001.

[114] T.M. Tritt, M.A. Subramanian, Thermoelectric materials, phenomena, and applications: A bird's eye view, MRS Bull. 31 (2006) 188–198. doi:10.1557/mrs2006.44.

[115] Springer handbook of nanotechnology, 2<sup>nd</sup> rev. & extended ed, Springer, Berlin ; New York, 2007.

[116] J.W. Gardner, Microsensors: principles and applications, Wiley, 1994.

[117] A. Majumdar, Thermoelectricity in semiconductor nanostructures, Science. 303 (2004) 777–778. doi:10.1126/science.1093164.

[118] G.J. Snyder, E.S. Toberer, Complex thermoelectric materials, Nat. Mater. 7 (2008) 105–114. doi:10.1038/nmat2090.

[119] C. Uher, Skutterudites: Prospective novel thermoelectrics, in: T.M. Tritt (Ed.), Semiconductors and Semimetals, Elsevier, San Diego, California, 2001: pp. 139–253. http://www.sciencedirect.com/science/article/pii/S0080878401801514 (accessed March 30, 2015).

[120] G.S. Nolas, G.A. Slack, S.B. Schujman, Semiconductor clathrates: A phonon glass electron crystal material with potential for thermoelectric applications, in: T.M. Tritt (Ed.), Semiconductors and Semimetals, Elsevier, San Diego, California, 2001: pp. 255–300. http://www.sciencedirect.com/science/article/pii/S0080878401801526 (accessed March 30, 2015).

[121] D.M. Rowe, ed., Thermoelectrics and its energy harvesting. Modules, sytems and applications in thermoelectrics, CRC Press, Boca Raton, FL, 2012. http://www.crcnetbase.com/doi/book/10.1201/b11892 (accessed November 15, 2013).

[122] V.L. Kuznetsov, L.A. Kuznetsova, A.E. Kaliazin, D.M. Rowe, Preparation and thermoelectric properties of AII 8BIII 16BIV 30 clathrate compounds, J. Appl. Phys. 87 (2000) 7871–7875. doi:10.1063/1.373469.

[123] G.S. Nolas, J.L. Cohn, G.A. Slack, S.B. Schujman, Semiconducting Ge clathrates: Promising candidates for thermoelectric applications, Appl. Phys. Lett. 73 (1998) 178–180. doi:10.1063/1.121747.

[124] G.S. Nolas, M. Kaeser, R.T. Littleton, T.M. Tritt, High figure of merit in partially filled ytterbium skutterudite materials, Appl. Phys. Lett. 77 (2000) 1855–1857. doi:10.1063/1.1311597.

[125] L.-D. Zhao, S.-H. Lo, Y. Zhang, H. Sun, G. Tan, C. Uher, C. Wolverton, V.P. Dravid, M.G. Kanatzidis, Ultralow thermal conductivity and high thermoelectric figure of merit in SnSe crystals, Nature. 508 (2014) 373–377. doi:10.1038/nature13184.

[126] D. Dávila, A. Tarancón, C. Calaza, M. Salleras, M. Fernández-Regúlez, A. San Paulo, L. Fonseca, Monolithically integrated thermoelectric energy harvester based on silicon nanowire arrays for powering micro/nanodevices, Nano Energy. 1 (2012) 812–819. doi:10.1016/j.nanoen.2012.06.006.

[127] K. Ziouche, Z. Yuan, P. Lejeune, T. Lasri, D. Leclercq, Z. Bougrioua, Silicon-Based Monolithic Planar Micro Thermoelectric Generator Using Bonding Technology, J. Microelectromech. Syst. 26 (2017) 45–47. doi:10.1109/JMEMS.2016.2633442.

[128] I. Chowdhury, R. Prasher, K. Lofgreen, G. Chrysler, S. Narasimhan, R. Mahajan, D. Koester, R. Alley, R. Venkatasubramanian, On-chip cooling by superlattice-based thin-film thermoelectrics, Nat. Nanotechnol. 4 (2009) 235–238. doi:10.1038/nnano.2008.417.

[129] L.M. Goncalves, J.G. Rocha, C. Couto, P. Alpuim, J.H. Correia, On-chip array of thermoelectric Peltier microcoolers, Sens. Actuators A: Phys. 145–146 (2008) 75–80. doi:10.1016/j.sna.2007.10.062.

[130] S.H. Choday, M.S. Lundstrom, K. Roy, Prospects of thin-film thermoelectric devices for hot-spot cooling and on-chip energy harvesting, IEEE Trans. Compon. Packag. Technol. 3 (2013) 2059–2067. doi:10.1109/TCPMT.2013.2273873.

[131] B. Poudel, Q. Hao, Y. Ma, Y. Lan, A. Minnich, B. Yu, X. Yan, D. Wang, A. Muto, D. Vashaee, X. Chen, J. Liu, M.S. Dresselhaus, G. Chen, Z. Ren, High-Thermoelectric Performance of Nanostructured Bismuth Antimony Telluride Bulk Alloys, Science. 320 (2008) 634–638. doi:10.1126/science.1156446.

[132] J.R. Sootsman, H. Kong, C. Uher, J.J. D'Angelo, C.-I. Wu, T.P. Hogan, T. Caillat, M.G. Kanatzidis, Large Enhancements in the Thermoelectric Power Factor of Bulk PbTe at High Temperature by Synergistic Nanostructuring, Angew. Chem. Int. Ed. 47 (2008) 8618–8622. doi:10.1002/anie.200803934.

[133] Q. Shen, L. Chen, T. Goto, T. Hirai, J. Yang, G.P. Meisner, C. Uher, Effects of partial substitution of Ni by Pd on the thermoelectric properties of ZrNiSn-based half-Heusler compounds, Appl. Phys. Lett. 79 (2001) 4165–4167. doi:10.1063/1.1425459.

[134] L.D. Chen, X.Y. Huang, M. Zhou, X. Shi, W.B. Zhang, The high temperature thermoelectric performances of $Zr_{0.5}Hf_{0.5}Ni_{0.8}Pd_{0.2}Sn_{0.99}Sb_{0.01}$ alloy with nanophase inclusions, J. Appl. Phys. 99 (2006) 064305. doi:10.1063/1.2180432.

[135] Z. Xiong, X. Chen, X. Huang, S. Bai, L. Chen, High thermoelectric performance of $Yb_{0.26}Co_4Sb_{12}/y$GaSb nanocomposites originating from scattering electrons of low energy, Acta Mater. 58 (2010) 3995–4002. doi:10.1016/j.actamat.2010.03.025.

[136] C.B. Vining, Silicon Germanium, in: CRC Handbook of Thermoelectrics, CRC Press, Boca Raton, FL, 1995: pp. 329–338.

[137] X.W. Wang, H. Lee, Y.C. Lan, G.H. Zhu, G. Joshi, D.Z. Wang, J. Yang, A.J. Muto, M.Y. Tang, J. Klatsky, S. Song, M.S. Dresselhaus, G. Chen, Z.F. Ren, Enhanced thermoelectric figure of merit in nanostructured n-type silicon germanium bulk alloy, Appl. Phys. Lett. 93 (2008) 193121. doi:10.1063/1.3027060.

[138] S.K. Bux, R.G. Blair, P.K. Gogna, H. Lee, G. Chen, M.S. Dresselhaus, R.B. Kaner, J.-P. Fleurial, Nanostructured bulk Silicon as an effective thermoelectric material, Adv. Funct. Mater. 19 (2009) 2445–2452. doi:10.1002/adfm.200900250.

[139] C. Uher, ed., Materials aspect of thermoelectricity, 1<sup>st</sup> edition, CRC Press, Boca Raton, 2016.

[140] T.M. Tritt, H. Böttner, L. Chen, Thermoelectrics: Direct solar thermal energy conversion, MRS Bull. 33 (2008) 366–368. doi:10.1557/mrs2008.73.

[141] R. Venkatasubramanian, E. Siivola, T. Colpitts, B. O'Quinn, Thin-film thermoelectric devices with high room-temperature figures of merit, Nature. 413 (2001) 597–602. doi:10.1038/35098012.

[142] K.F. Hsu, Cubic $AgPb_mSbTe_{2+m}$: Bulk Thermoelectric Materials with High Figure of Merit, Science. 303 (2004) 818–821. doi:10.1126/science.1092963.

[143] A.T. Duong, V.Q. Nguyen, G. Duvjir, V.T. Duong, S. Kwon, J.Y. Song, J.K. Lee, J.E. Lee, S. Park, T. Min, J. Lee, J. Kim, S. Cho, Achieving ZT=2.2 with Bi-doped *n*-type SnSe single crystals, Nat Commun. 7 (2016) 13713. doi:10.1038/ncomms13713.

[144] H.J. Goldsmid, A.R. Sheard, D.A. Wright, The performance of bismuth telluride thermojunctions, Br. J. Appl. Phys. 9 (1958) 365. doi:10.1088/0508-3443/9/9/306.

[145] D.-Y. Chung, T. Hogan, P. Brazis, M. Rocci-Lane, C. Kannewurf, M. Bastea, C. Uher, M.G. Kanatzidis, $CsBi_4Te_6$: A High-Performance Thermoelectric Material for Low-Temperature Applications, Science. 287 (2000) 1024–1027. doi:10.1126/science.287.5455.1024.

[146] X. Yan, B. Poudel, Y. Ma, W.S. Liu, G. Joshi, H. Wang, Y. Lan, D. Wang, G. Chen, Z.F. Ren, Experimental Studies on Anisotropic Thermoelectric Properties and Structures of n-Type $Bi_2Te_{2.7}Se_{0.3}$, Nano Lett. 10 (2010) 3373–3378. doi:10.1021/nl101156v.

[147] A.F. Joffe, L.S. Stil'bans, Physical problems of thermoelectricity, Rep. Prog. Phys. 22 (1959) 167. doi:10.1088/0034-4885/22/1/306.

[148] P.F.P. Poudeu, J. D'Angelo, A.D. Downey, J.L. Short, T.P. Hogan, M.G. Kanatzidis, High Thermoelectric Figure of Merit and Nanostructuring in Bulk p-type $Na_{1-x}Pb_mSb_yTe_{m+2}$, Angew. Chem. Int. Ed. 45 (2006) 3835–3839. doi:10.1002/anie.200600865.

[149] T. Caillat, J.-P. Fleurial, A. Borshchevsky, Preparation and thermoelectric properties of semiconducting $Zn_4Sb_3$, J. Phys. Chem. Solids. 58 (1997) 1119–1125. doi:10.1016/S0022-3697(96)00228-4.

[150] J. Davidow, Y. Gelbstein, A Comparison Between the Mechanical and Thermoelectric Properties of Three Highly Efficient *p*-Type GeTe-Rich Compositions: TAGS-80, TAGS-85, and 3% $Bi_2Te_3$-Doped $Ge_{0.87}Pb_{0.13}Te$, J. Electron. Mater. 42 (2013) 1542–1549. doi:10.1007/s11664-012-2316-y.

[151] J. Zhang, L. Song, S.H. Pedersen, H. Yin, L.T. Hung, B.B. Iversen, Discovery of high-performance low-cost n-type $Mg_3Sb_2$-based thermoelectric materials with multi-valley conduction bands, Nat. Commun. 8 (2017) 13901. doi:10.1038/ncomms13901.

[152] C. Wood, Materials for thermoelectric energy conversion, Rep. Prog. Phys. 51 (1988) 459. doi:10.1088/0034-4885/51/4/001.

[153] X. Tang, Q. Zhang, L. Chen, T. Goto, T. Hirai, Synthesis and thermoelectric properties of p-type- and n-type-filled skutterudite $R_yM_xCo_{4-x}Sb_{12}$(R:Ce,Ba,Y;M:Fe,Ni), J. Appl. Phys. 97 (2005) 093712. doi:10.1063/1.1888048.

[154] A.F. May, E.S. Toberer, A. Saramat, G.J. Snyder, Characterization and analysis of thermoelectric transport in *n*-type $Ba_8Ga_{16-x}Ge_{30+x}$, Phys. Rev. B. 80 (2009). doi:10.1103/PhysRevB.80.125205.

[155] J. Shuai, H. Geng, Y. Lan, Z. Zhu, C. Wang, Z. Liu, J. Bao, C.-W. Chu, J. Sui, Z. Ren, Higher thermoelectric performance of Zintl phases $(Eu_{0.5}Yb_{0.5})_{1-x}Ca_xMg_2Bi_2$ by band engineering and strain fluctuation, Proc. Natl. Acad. Sci. U.S.A. 113 (2016) E4125–E4132. doi:10.1073/pnas.1608794113.

[156] M.S. Dresselhaus, G. Chen, M.Y. Tang, R.G. Yang, H. Lee, D.Z. Wang, Z.F. Ren, J.-P. Fleurial, P. Gogna, New Directions for Low-Dimensional Thermoelectric Materials, Adv. Mater. 19 (2007) 1043–1053. doi:10.1002/adma.200600527.

[157] G. Joshi, H. Lee, Y. Lan, X. Wang, G. Zhu, D. Wang, R.W. Gould, D.C. Cuff, M.Y. Tang, M.S. Dresselhaus, G. Chen, Z. Ren, Enhanced Thermoelectric Figure-of-Merit in Nanostructured p-type Silicon Germanium Bulk Alloys, Nano Lett. 8 (2008) 4670–4674. doi:10.1021/nl8026795.

[158] C. Fu, S. Bai, Y. Liu, Y. Tang, L. Chen, X. Zhao, T. Zhu, Realizing high figure of merit in heavy-band *p*-type half-Heusler thermoelectric materials, Nat. Commun. 6 (2015) 8144. doi:10.1038/ncomms9144.

[159] M. Strasser, R. Aigner, M. Franosch, G. Wachutka, Miniaturized thermoelectric generators based on poly-Si and poly-SiGe surface micromachining, Sens. Actuators A: Phys. 97–98 (2002) 535–542. doi:10.1016/s0924-4247(01)00815-9.

[160] M. Strasser, R. Aigner, C. Lauterbach, T.F. Sturm, M. Franosch, G.K.M. Wachutka, Micromachined CMOS thermoelectric generators as on-chip power supply, Sens. Actuators A: Phys. 114 (2004) 362–370. doi:10.1016/j.sna.2003.11.039.

[161] S.M. Yang, M. Cong, T. Lee, Application of quantum well-like thermocouple to thermoelectric energy harvester by BiCMOS process, Sensors and Actuators A: Physical. 166 (2011) 117–124. doi:10.1016/j.sna.2010.06.031.

[162] J. Xie, C. Lee, H. Feng, Design, Fabrication, and Characterization of CMOS MEMS-Based Thermoelectric Power Generators, J. Microelectromech. Syst. 19 (2010) 317–324. doi:10.1109/JMEMS.2010.2041035.

[163] X. Yu, Y. Wang, Y. Liu, T. Li, H. Zhou, X. Gao, F. Feng, T. Roinila, Y. Wang, CMOS MEMS-based thermoelectric generator with an efficient heat dissipation path, J. Micromech. Microeng. 22 (2012) 105011. doi:10.1088/0960-1317/22/10/105011.

[164] Z. Wang, Y. van Andel, M. Jambunathan, V. Leonov, R. Elfrink, R.J.M. Vullers, Characterization of a Bulk-Micromachined Membraneless In-Plane Thermopile, J. Electron. Mater. 40 (2011) 499–503. doi:10.1007/s11664-010-1402-2.

[165] A.P. Perez-Marín, A.F. Lopeandía, L. Abad, P. Ferrando-Villaba, G. Garcia, A.M. Lopez, F.X. Muñoz-Pascual, J. Rodríguez-Viejo, Micropower thermoelectric generator from thin Si membranes, Nano Energy. 4 (2014) 73–80. doi:10.1016/j.nanoen.2013.12.007.

[166] E. Hourdakis, A.G. Nassiopoulou, A Thermoelectric Generator Using Porous Si Thermal Isolation, Sensors. 13 (2013) 13596–13608. doi:10.3390/s131013596.

[167] Y. Li, K. Buddharaju, B.C. Tinh, N. Singh, S.J. Lee, Improved Vertical Silicon Nanowire Based Thermoelectric Power Generator With Polyimide Filling, IEEE Electron Device Lett. 33 (2012) 715–717. doi:10.1109/LED.2012.2187424.

[168] V. Leonov, Y. van Andel, Z. Wang, R.J.M. Vullers, C. Van Hoof, Micromachined polycrystalline Si thermopiles in a T-shirt, Sensors and Transducers. 127 (2011) 15–26.

[169] B.M. Curtin, E.W. Fang, J.E. Bowers, Highly Ordered Vertical Silicon Nanowire Array Composite Thin Films for Thermoelectric Devices, J. Electron. Mater. 41 (2012) 887–894. doi:10.1007/s11664-012-1904-1.

[170] M. Wagner, G. Span, S. Holzer, T. Grasser, Thermoelectric power generation using large-area Si/SiGe pn-junctions with varying Ge content, Semicond. Sci. Technol. 22 (2007) S173. doi:10.1088/0268-1242/22/1/s41.

[171] G. Span, M. Wagner, T. Grasser, Thermoelectric power generation using large area pn-junctions, in: The 3[Rd] European Conference on Thermoelectrics Proceedings ECT2005, Nancy, France, 2005: pp. 72–75.

[172] J.H. Kiely, D.-H. Lee, Characteristics of $Bi_{0.5}Sb_{1.5}Te_3/Be_2Te_{2.4}Se_{0.6}$ thin-film thermoelectric devices for power generation, Meas. Sci. Technol. 8 (1997) 661. doi:10.1088/0957-0233/8/6/013.

[173] M. Stordeur, I. Stark, Low power thermoelectric generator-self-sufficient energy supply for micro systems, in: 16[Th] International Conference on Thermoelectrics, 1997. Proceedings ICT '97, IEEE, Dresden, Germany, 1997: pp. 575–577. doi:10.1109/ICT.1997.667595.

[174] I.-H. Kim, $(Bi,Sb)_2(Te,Se)_3$-based thin film thermoelectric generators, Mater. Lett. 43 (2000) 221–224. doi:10.1016/S0167-577X(99)00239-6.

[175] G.J. Snyder, J.R. Lim, C.-K. Huang, J.-P. Fleurial, Thermoelectric microdevice fabricated by a MEMS-like electrochemical process, Nat. Mater. 2 (2003) 528. doi:10.1038/nmat943.

[176] V. Leonov, P. Fiorini, S. Sedky, T. Torfs, C. Van Hoof, Thermoelectric mems generators as a power supply for a body area network, in: The 13[Th] International Conference on Solid-State Sensors, Actuators and Microsystems, TRANSDUCERS'05. Digest of Technical Papers, IEEE, Seoul, South Korea, 2005: pp. 291–294. doi:10.1109/SENSOR.2005.1496414.

[177] V. Leonov, T. Torfs, P. Fiorini, C. Van Hoof, Thermoelectric Converters of Human Warmth for Self-Powered Wireless Sensor Nodes, IEEE Sens. J. 7 (2007) 650–657. doi:10.1109/JSEN.2007.894917.

[178] W. Glatz, E. Schwyter, L. Durrer, C. Hierold, $Bi_2Te_3$-Based Flexible Micro Thermoelectric Generator With Optimized Design, J. Microelectromech. Syst. 18 (2009) 763–772. doi:10.1109/JMEMS.2009.2021104.

[179] R. Roth, R. Rostek, K. Cobry, C. Kohler, M. Groh, P. Woias, Design and Characterization of Micro Thermoelectric Cross-Plane Generators With Electroplated $Bi_2Te_3$, $Sb_xTe_y$, and Reflow Soldering, J. Micromech. Syst. 23 (2014) 961–971. doi:10.1109/JMEMS.2014.2303198.

[180] H. Glosch, M. Ashauer, U. Pfeiffer, W. Lang, A thermoelectric converter for energy supply, Sens. Actuators A: Phys. 74 (1999) 246–250. doi:10.1016/S0924-4247(98)00298-2.

[181] M. Kishi, H. Nemoto, T. Hamao, M. Yamamoto, S. Sudou, M. Mandai, S. Yamamoto, Micro thermoelectric modules and their application to wristwatches as an energy source, in: 18[Th] International Conference on Thermoelectrics, IEEE, Baltimore, MD, USA, 1999: pp. 301–307. doi:10.1109/ICT.1999.843389.

[182] H. Bottner, J. Nurnus, A. Gavrikov, G. Kuhner, M. Jagle, C. Kunzel, D. Eberhard, G. Plescher, A. Schubert, K.-H. Schlereth, New thermoelectric components using microsystem technologies, J. Microelectromech. Syst. 13 (2004) 414–420. doi:10.1109/JMEMS.2004.828740.

[183] N. Ghafouri, H. Kim, M.Z. Atashbar, K. Najafi, A micro thermoelectric energy scavenger for a hybrid insect, in: 2008 IEEE Sensors, IEEE, Lecce, Italy, 2008: pp. 1249–1252. doi:10.1109/ICSENS.2008.4716670.

[184] T.C. Harman, R.E. Reeder, M.P. Walsh, B.E. LaForge, C.D. Hoyt, G.W. Turner, High electrical power density from PbTe-based quantum-dot superlattice unicouple thermoelectric devices, Appl. Phys. Lett. 88 (2006) 243504. doi:10.1063/1.2209707.

[185] J. Su, V. Leonov, M. Goedbloed, Y. van Andel, M.C. de Nooijer, R. Elfrink, Z. Wang, R.J.M. Vullers, A batch process micromachined thermoelectric energy harvester: fabrication and characterization, J. Micromech. Microeng. 20 (2010) 104005. doi:10.1088/0960-1317/20/10/104005.

[186] T. Huesgen, P. Woias, N. Kockmann, Design and fabrication of MEMS thermoelectric generators with high temperature efficiency, Sens. Actuators A: Phys. 145–146 (2008) 423–429. doi:10.1016/j.sna.2007.11.032.

[187] M. Takashiri, T. Shirakawa, K. Miyazaki, H. Tsukamoto, Fabrication and characterization of bismuth–telluride-based alloy thin film thermoelectric generators by flash evaporation method, Sens. Actuators A: Phys. 138 (2007) 329–334. doi:10.1016/j.sna.2007.05.030.

[188] H. Bottner, J. Nurnus, A. Schubert, F. Volkert, New high density micro structured thermogenerators for stand alone sensor systems, in: 26[Th] International Conference on Thermoelectrics, IEEE, Jeju Island, South Korea, 2007: pp. 306–309. doi:10.1109/ICT.2007.4569484.

[189] H. Scherrer, S. Scherrer, Bismuth Telluride, Antimony Telluride and their solid solutions, in: CRC Handbook of Thermoelectrics, CRC Press, Boca Raton, FL, 1995.

[190] V. Fano, Lead telluride and its alloys, in: CRC Handbook of Thermoelectrics, CRC Press, Boca Raton, FL, 1995.

[191] U.S. Geological Survey, Mineral commodities summary 2018, U.S. Government printing office, Reston, Virginia, 2018.

[192] M. Haras, V. Lacatena, T.M. Bah, S. Didenko, J.F. Robillard, S. Monfray, T. Skotnicki, E. Dubois, Fabrication of thin-film silicon membranes with phononic crystals for thermal conductivity measurements, IEEE Electron Device Lett. 37 (2016) 1358–1361. doi:10.1109/LED.2016.2600590.

[193] M. Haras, V. Lacatena, F. Morini, J.-F. Robillard, S. Monfray, T. Skotnicki, E. Dubois, Fabrication of integrated micrometer platform for thermoelectric measurements, in: Technical Digest - International Electron Devices Meeting (IEDM), San Francisco, California, 2014: pp. 8.5.212-8.5.215. doi:10.1109/IEDM.2014.7047012.

[194] W. Liu, M. Asheghi, Phonon–boundary scattering in ultrathin single-crystal silicon layers, Appl. Phys. Lett. 84 (2004) 3819. doi:10.1063/1.1741039.

[195] J. Cuffe, E. Chávez, A. Shchepetov, P.-O. Chapuis, E.H. El Boudouti, F. Alzina, T. Kehoe, J. Gomis-Bresco, D. Dudek, Y. Pennec, B. Djafari-Rouhani, M. Prunnila, J. Ahopelto, C.M. Sotomayor Torres, Phonons in Slow Motion: Dispersion Relations in Ultrathin Si Membranes, Nano Lett. 12 (2012) 3569–3573. doi:10.1021/nl301204u.

[196] P.E. Hopkins, C.M. Reinke, M.F. Su, R.H. Olsson, E.A. Shaner, Z.C. Leseman, J.R. Serrano, L.M. Phinney, I. El-Kady, Reduction in the thermal conductivity of single crystalline Silicon by phononic crystal patterning, Nano Lett. 11 (2011) 107–112. doi:10.1021/nl102918q.

[197] J.-K. Yu, S. Mitrovic, D. Tham, J. Varghese, J.R. Heath, Reduction of thermal conductivity in phononic nanomesh structures, Nat. Nanotechnol. 5 (2010) 718–721. doi:10.1038/nnano.2010.149.

[198] B. Graczykowski, A. El Sachat, J.S. Reparaz, M. Sledzinska, M.R. Wagner, E. Chavez-Angel, Y. Wu, S. Volz, Y. Wu, F. Alzina, C.M. Sotomayor Torres, Thermal conductivity and air-mediated losses in periodic porous silicon membranes at high temperatures, Nat. Commun. 8 (2017). doi:10.1038/s41467-017-00115-4.

[199] M.R. Wagner, B. Graczykowski, J.S. Reparaz, A. El Sachat, M. Sledzinska, F. Alzina, C.M. Sotomayor Torres, Two-Dimensional Phononic Crystals: Disorder Matters, Nano Lett. 16 (2016) 5661–5668. doi:10.1021/acs.nanolett.6b02305.

[200] S. Volz, J. Ordonez-Miranda, A. Shchepetov, M. Prunnila, J. Ahopelto, T. Pezeril, G. Vaudel, V. Gusev, P. Ruello, E.M. Weig, M. Schubert, M. Hettich, M. Grossman, T. Dekorsy, F. Alzina, B. Graczykowski, E. Chavez-Angel, J.S. Reparaz, M.R. Wagner, C.M. Sotomayor-Torres, S. Xiong, S. Neogi, D. Donadio, Nanophononics: state of the art and perspectives, Eur. Phys. J. B. 89 (2016) 15. doi:10.1140/epjb/e2015-60727-7.

[201] J. Tang, H.-T. Wang, D.H. Lee, M. Fardy, Z. Huo, T.P. Russell, P. Yang, Holey Silicon as an Efficient Thermoelectric Material, Nano Lett. 10 (2010) 4279–4283. doi:10.1021/nl102931z.

[202] M. Haras, V. Lacatena, F. Morini, J.-F. Robillard, S. Monfray, T. Skotnicki, E. Dubois, Thermoelectric energy conversion: How good can silicon be?, Mater. Lett. 157 (2015) 193–196. doi:10.1016/j.matlet.2015.05.012.

[203] M. Haras, Thermoelectric energy conversion based on thin-film Silicon technology, Éditions Universitaires Européennes, Saarbrücken, 2016. http://nbn-resolving.de/urn:nbn:de:101:1-201610206507 (accessed November 10, 2016).

[204] R. Stobart, Z. Yang, S. Lan, System Design Considerations for Thermoelectric Energy Recovery, in: Thermoelectric Materials and Devices, Royal Society of Chemistry, Cambridge, 2017: pp. 156–203. doi:10.1039/9781782624042-00156.

[205] H. Edwards, J. Debord, T. Tran, D. Freeman, K. Maggio, A Theory of Thermoelectric Energy Harvesting Systems, in: Innovative Materials and Systems for Energy Harvesting Applications:, IGI Global, Hershey, PA, USA, 2015: pp. 254–270. doi:10.4018/978-1-4666-8254-2.

[206] M. Di Paolo Emilio, Powering Microsystem, in: Microelectronic Circuit Design for Energy Harvesting Systems, Springer International Publishing, Cham, 2017: pp. 75–104. doi:10.1007/978-3-319-47587-5_8.

[207] J. Bierschenk, Optimized thermoelectrics for energy harvesting applications, in: Applications of Ferroelectrics, 2008. ISAF 2008. 17Th IEEE International Symposium on The, 2008: pp. 1–4. doi:10.1109/ISAF.2008.4693950.

[208] G.S. Nolas, Thermoelectrics: basic principles and new materials developments, Springer, Berlin ; New York, 2001.

[209] R.R. Heikes, R.W. Ure, Thermoelectricity: science and engineering, Interscience Publishers, New York, NY, 1961.

[210] S. Lineykin, S. Ben-Yaakov, SPICE compatible equivalent circuit of the energy conversion processes in thermoelectric modules, in: Proceedings of the 23Rd IEEE Convention of Electrical and Electronics Engineers, Israel, 2004: pp. 346–349. doi:10.1109/EEEI.2004.1361162.

[211] K. Itoigawa, H. Ueno, M. Shiozaki, T. Toriyama, S. Sugiyama, Fabrication of flexible thermopile generator, J. Micromech. Microeng. 15 (2005) S233–S238. doi:10.1088/0960-1317/15/9/S10.

[212] S. Hasebe, J. Ogawa, T. Toriyama, S. Sugiyama, H. Ueno, K. Itoigawa, Design and Fabrication of flexible thermopile for power generation, in: Micromechatronics and Human Science, 2003. MHS 2003. Proceedings of 2003 International Symposium On, IEEE, Nagoya, Japan, 2003: pp. 287–291. doi:10.1109/MHS.2003.1249950.

[213] E.T. Topal, H. Kulah, A. Muhtaroglu, Thin film thermoelectric energy harvesters for MEMS micropower generation, in: 2010 International Conference on Energy Aware Computing, 2010: pp. 1–4. doi:10.1109/ICEAC.2010.5702321.

[214] S.Y. (Ron) Hui, H.S.H. Chung, Resonant and Soft-switching Converters, in: Power Electronics Handbook, Elsevier, 2011: pp. 409–453. doi:10.1016/B978-0-12-382036-5.00016-1.

[215] N. Mohan, Power electronics: a first course, Wiley, Hoboken, N.J, 2012.

[216] Linear Technology Corporation, LTC3108 - Ultralow Voltage Step-Up Converter and Power Manager, (2009). http://www.analog.com/media/en/technical-documentation/data-sheets/3108fc.pdf (accessed April 11, 2018).

[217] Linear Technology Corporation, LTC3588-2 - Nanopower Energy Harvesting Power Supply, (2010). http://www.analog.com/media/en/technical-documentation/data-sheets/35881fc.pdf (accessed April 11, 2018).

[218] Texas Instruments, Inc., BQ25570 - Ultra Low Power Harvester Power Management IC with Boost Charger, (2011). http://www.ti.com/lit/ds/symlink/bq25570.pdf.

[219] Texas Instruments, Inc., BQ25505 -Ultra Low Power Boost Converter with Battery Management, (2015). http://www.ti.com/lit/ds/symlink/bq25505.pdf.

[220] Analog Devices, Inc., ADP5092 -Ultralow Power Energy Harvester PMU with MPPT and Charge Management, (2017). http://www.analog.com/media/en/technical-documentation/data-sheets/ADP5091-5092.pdf.

[221] STMicroelectronics, SPV1050 - Ultralow power energy harvester and battery charger, (2015). http://www.st.com/content/ccc/resource/technical/document/datasheet/3e/91/0f/7c/32/3e/46/dd/DM00100984.pdf/files/DM00100984.pdf/jcr:content/translations/en.DM00100984.pdf (accessed April 11, 2018).

[222] Linear Technology Corporation, LTC3106 - 300mA Low Voltage Buck-Boost Converter with PowerPath and 1.6µA Quiescent Current, (2015). http://www.analog.com/media/en/technical-documentation/data-sheets/3106f.pdf.

[223] Analog Devices, Inc., ADP5304 -Ultralow Power Step-Down Regulator for Energy Harvesting, (2015). http://www.analog.com/media/en/technical-documentation/data-sheets/ADP5304.pdf.

[224] Cypress Semiconductor Corporation, S6AE101A - Energy Harvesting PMIC for Wireless Sensor Node, (2017). http://www.cypress.com/file/219311/download (accessed April 11, 2018).

[225] Linear Technology Corporation, LTC3109 - Auto-Polarity, Ultralow Voltage Step-Up Converter and Power Manager, (2013). http://www.analog.com/media/en/technical-documentation/data-sheets/3109fb.pdf.

[226] I. Doms, P. Merken, C.V. Hoof, R.P. Mertens, Capacitive Power Management Circuit for Micropower Thermoelectric Generators With a 1.4 µA Controller, IEEE J. Solid-State Circuits. 44 (2009) 2824–2833. doi:10.1109/JSSC.2009.2027546.

[227] Y.K. Ramadass, A.P. Chandrakasan, A Battery-Less Thermoelectric Energy Harvesting Interface Circuit With 35 mV Startup Voltage, IEEE J. Solid-State Circuits. 46 (2011) 333–341. doi:10.1109/JSSC.2010.2074090.

[228] P.S. Weng, H.Y. Tang, P.C. Ku, L.H. Lu, 50 mV-Input Batteryless Boost Converter for Thermal Energy Harvesting, IEEE J. Solid-State Circuits. 48 (2013) 1031–1041. doi:10.1109/JSSC.2013.2237998.

[229] J. Kim, C. Kim, A DC-DC Boost Converter With Variation-Tolerant MPPT Technique and Efficient ZCS Circuit for Thermoelectric Energy Harvesting Applications, IEEE Trans. Power Electron. 28 (2013) 3827–3833. doi:10.1109/TPEL.2012.2231098.

[230] E.E. Aktakka, K. Najafi, A Micro Inertial Energy Harvesting Platform With Self-Supplied Power Management Circuit for Autonomous Wireless Sensor Nodes, IEEE J. Solid-State Circuits. 49 (2014) 2017–2029. doi:10.1109/JSSC.2014.2331953.

[231] S. Bandyopadhyay, P.P. Mercier, A.C. Lysaght, K.M. Stankovic, A.P. Chandrakasan, A 1.1 nW Energy-Harvesting System with 544 pW Quiescent Power for Next-Generation Implants, IEEE J. Solid-State Circuits. 49 (2014) 2812–2824. doi:10.1109/JSSC.2014.2350260.

[232] W. Jung, S. Oh, S. Bang, Y. Lee, D. Sylvester, D. Blaauw, 23.3 A 3nW fully integrated energy harvester based on self-oscillating switched-capacitor DC-DC converter, in: 2014 IEEE International Solid-State Circuits Conference Digest of Technical Papers (ISSCC), IEEE, San Francisco, CA, USA, 2014: pp. 398–399. doi:10.1109/ISSCC.2014.6757486.

[233] P.C. Dias, F.J.O. Morais, M.B. de M. França, E.C. Ferreira, A. Cabot, J.A.S. Dias, Autonomous Multisensor System Powered by a Solar Thermoelectric Energy Harvester With Ultralow-Power Management Circuit, IEEE Trans. Instrum. Meas. 64 (2015) 2918–2925. doi:10.1109/TIM.2015.2444253.

[234] Y. Toyama, T. Ogawa, T. Ueno, T. Itakura, 20 mV input, 4.2 V output SIDO boost converter with low-power controller and adaptive switch size selector for thermoelectric energy harvesting, in: 2016 IEEE Asian Solid-State Circuits Conference (A-SSCC), IEEE, Toyama, Japan, 2016: pp. 9–12. doi:10.1109/ASSCC.2016.7844122.

[235] A.A. Blanco, G.A. Rincón-Mora, Compact Fast-Waking Light/Heat-Harvesting 0.18-µm CMOS Switched-Inductor Charger, IEEE Trans. Circuits Syst. I Regul. Pap. 65 (2018) 2024–2034. doi:10.1109/TCSI.2017.2766188.

[236] M. Dini, A. Romani, M. Filippi, M. Tartagni, A Nanocurrent Power Management IC for Low-Voltage Energy Harvesting Sources, IEEE Trans. Power Electron. 31 (2016) 4292–4304. doi:10.1109/TPEL.2015.2472480.

[237] K. Rawy, T. Yoo, T.T.H. Kim, An 88% Efficiency 0.1-300µW Energy Harvesting System With 3-D MPPT Using Switch Width Modulation for IoT Smart Nodes, IEEE J. Solid-State Circuits. (2018) 1–12. doi:10.1109/JSSC.2018.2833278.

[238] Sensirion AG, SGP30 Sensirion Gas Platform, (2017). https://www.sensirion.com/fileadmin/user_upload/customers/sensirion/Dokumente/0_Datasheets/Gas/Sensirion_Gas_Sensors_SGP30_Datasheet.pdf.

[239] Bosch Sensortec GmbH, BME680 - Low power gas, pressure, temperature & humidity sensor, (2017). https://ae-bst.resource.bosch.com/media/_tech/media/datasheets/BST-BME680-DS001-00.pdf.

[240] Amphenol Corp., T6713 Series $CO_2$ Module, (2017). https://www.amphenol-sensors.com/en/component/edocman/297-t6713-datasheet/download?Itemid=.

[241] ams AG, iAQ-Core Indoor Air Quality Sensor Module, (2015). https://ams.com/documents/20143/36005/iAQ-core_DS000334_1-00.pdf.

[242] Silicon Laboratories Inc., Si7050/1/3/4/5-A20 $I^2C$ temperature sensors, (2016). https://www.silabs.com/documents/public/data-sheets/Si7050-1-3-4-5-A20.pdf.

[243] NXP Semiconductors N.V., PCT2075 - $I^2C$-bus Fm+, 1°C accuracy, digital temperature sensor and thermal watchdog, (2013). https://www.nxp.com/docs/en/data-sheet/PCT2075.pdf.

[244] ROHM Semiconductor Co., Ltd., BD1020HFV - Temperature Sensor IC Analog Output, (2015). https://www.rohm.com/datasheet/BD1020HFV/bd1020hfv-e.

[245] Texas Instruments, Inc., TMP20 ±2.5°C Low-Power, Analog Out Temperature Sensor, (2009). http://www.ti.com/lit/ds/symlink/tmp20.pdf.

[246] Texas Instruments, Inc., LMT84 1.5 V, SC70/TO-92/TO-92S, Analog Temperature Sensors, (2013). http://www.ti.com/lit/ds/symlink/lmt84.pdf.

[247] Atmel Corporation, AT30TSE752A, AT30TSE754A, AT30TSE758A - 9-to-12-bit Selectable, ±0.5°C Accurate Digital Temperature Sensor with Nonvolatile Registers and Serial EEPROM, (2013). http://ww1.microchip.com/downloads/en/DeviceDoc/Atmel-8854-DTS-AT30TSE752A-754A-758A-Datasheet.pdf.

[248] Analog Devices, Inc., ADUX1020 - Photometric Sensor for Gesture and Proximity, (2016). http://www.analog.com/media/en/technical-documentation/data-sheets/ADUX1020.pdf.

[249] Analog Devices, Inc., ADPD188GG - Integrated Optical Module with Ambient Light Rejection and Two LEDs, (2018). http://www.analog.com/media/en/technical-documentation/data-sheets/adpd188gg.pdf.

[250] Texas Instruments, Inc., FDC2112-Q1, FDC2114-Q1, FDC2212-Q1, FDC2214-Q1 Multi-Channel 12-Bit or 28-Bit Capacitance-to-Digital Converter (FDC) for Capacitive Sensing, (2016). http://www.ti.com/lit/ds/symlink/fdc2214-q1.pdf.

[251] STMicroelectronics, VL6180X - Proximity and ambient light sensing (ALS) module, (2013). https://www.st.com/resource/en/datasheet/vl6180x.pdf.

[252] STMicroelectronics, VL53L1X - A new generation, long distance ranging Time-of-Flight sensor based on ST's FlightSense™ technology, (2018). https://www.st.com/resource/en/datasheet/vl53l1x.pdf.

[253] ON Semiconductor, NOA1212 - Ambient Light Sensor with Dark Current Compensation, (2017). http://www.onsemi.com/pub/Collateral/NOA1212-D.PDF.

[254] Texas Instruments, Inc., OPT3007 Ultra-Thin Ambient Light Sensor, (2017). http://www.ti.com/lit/ds/symlink/opt3007.pdf.

[255] Maxim Integrated Products, MAX30105 - High-Sensitivity Optical Sensor for Smoke Detection Applications, (2016). https://datasheets.maximintegrated.com/en/ds/MAX30105.pdf.

[256] Microchip Technology Inc., RE46C190 - CMOS Low Voltage Photoelect ric Smoke Detector ASIC with Interconnect and Timer Mode, (2010). http://ww1.microchip.com/downloads/en/DeviceDoc/22271A.pdf.

[257] NXP Semiconductors N.V., MPX53 - 0 to 50 kPa, Differential and Gauge, Uncompensated, Silicon Pressure Sensors, (2015). https://www.nxp.com/docs/en/data-sheet/MPX53.pdf.

[258] NXP Semiconductors N.V., FXPQ3115BV - I$^2$C precision pressure sensor with altimetry, (2017). https://www.nxp.com/docs/en/data-sheet/FXPQ3115BVSDS.pdf.

[259] Silicon Microstructures, Inc., SM5420E Series - Small Absolute Pressure Sensor, (2016). https://www.si-micro.com/fileadmin/00_smi_relaunch/products/uncompensated/datasheets/SM5420_Datasheet.pdf.

[260] TE Connectivity, MS5561C - Micro Altimeter, (2017). http://www.te.com/commerce/DocumentDelivery/DDEController?Action=showdoc&DocId=Data+Sheet%7FMS5561C%7FA3%7Fpdf%7FEnglish%7FENG_DS_MS5561C_A3.pdf%7FCAT-BLPS0034.

[261] STMicroelectronics, LPS25H - MEMS pressure sensor: 260-1260hPa absolute digital output barometer, (2013). https://www.st.com/resource/en/datasheet/lps25h.pdf.

[262] STMicroelectronics, LPS33HW - MEMS pressure sensor: 260-1260 hPa absolute digital output barometer with water-resistant package, (2017). https://www.st.com/resource/en/datasheet/lps33hw.pdf.

[263] STMicroelectronics, LPS35HW - MEMS pressure sensor: 260- 1260hPa absolute digital output barometer with water resistant package, (2016). https://www.st.com/resource/en/datasheet/lps35hw.pdf.

[264] Bosch Sensortec GmbH, BMP388 - Digital pressure sensor, (2016). https://ae-bst.resource.bosch.com/media/_tech/media/datasheets/BST-BMP388-DS001-01.pdf.

[265] NXP Semiconductors N.V., MPL115A2 - Miniature I $^2$C digital barometer, 50 to 115 kPa, (2012). https://www.nxp.com/docs/en/data-sheet/MPL115A2.pdf.

[266] Vishay Semiconductors, TSSP57038 - IR Receiver Modules for Remote Control Systems, (2018). https://www.vishay.com/docs/82482/tssp57038.pdf.

[267] Fairchild Semiconductor Corp., FLD00042 - I$^2$C Digital Ambient Light Sensor, (2012). http://pdf.datasheetcatalog.com/datasheet/fairchildsemiconductor/FLD00042.pdf.

[268] Intersil Corp., ISL29033 - Ultra-Low Lux, Low Power, Integrated Digital Ambient Light Sensor with Interrupt Function, (2011). https://www.intersil.com/content/dam/intersil/documents/isl2/isl29033.pdf.

[269] Maxim Integrated Products, MAX44004 - Digital Ambient Light Sensor, (2012). https://datasheets.maximintegrated.com/en/ds/MAX44004.pdf.

[270] J. Happich, Steep growth for thermoelectric energy harvesting, says Infinergia Consulting, EDN Europe. (2014). http://www.power-eetimes.com/en/steep-growth-for-thermoelectric-energy-harvesting-says-infinergia-consulting.html?cmp_id=7&news_id=222908168 (accessed March 20, 2015).

[271] Sub-Watt Thermoelectric Energy Harvesting Industry & Market Report, INFINERGIA Consulting, Grenoble, France, 2016. https://www.infinergia.com/en/energy-harvesting#sub-watt-thermoelectric (accessed September 6, 2018).

[272] Micropelt GmbH, Self-powered Thermostatic Radiator Valve, iTRV Type MVA-002, (2017). http://www.micropelt.com/fileadmin/user_upload/_PDF_MVA002_User_guide_EN.pdf (accessed September 6, 2018).

[273] Micropelt GmbH, Wireless heating valve actuator MVA003 EnOcean, (2017). http://www.micropelt.com/fileadmin/user_upload/_PDF_MVA003_Datasheet_1DSMVA003_0217v7e.pdf (accessed September 6, 2018).

[274] Micropelt GmbH, Wireless heating valve actuator MVA004 EnOcean, (2017). http://www.micropelt.com/fileadmin/user_upload/_PDF_MVA004_datasheet_1DSMVA004_0817v11e.pdf (accessed September 6, 2018).

[275] J. Liebl, S. Neugebauer, A. Eder, M. Linde, B. Mazar, W. Stütz, The thermoelectric generator from BMW is making use of waste heat, MTZ Worldw. 70 (2009) 4–11. doi:10.1007/BF03226939.

[276] B. Silke, Looking for the next gram. BMW EfficientDynamics means ongoing research. Exhaust heat offers the greatest potential for the future., BMW Group. (2011). https://www.press.bmwgroup.com/global/article/detail/T0119738EN/looking-for-the-next-gram?language=en (accessed March 11, 2018).

[277] B. Orr, A. Akbarzadeh, M. Mochizuki, R. Singh, A review of car waste heat recovery systems utilising thermoelectric generators and heat pipes, Applied Thermal Engineering. 101 (2016) 490–495. doi:10.1016/j.applthermaleng.2015.10.081.

[278] K.J. Heilman, S.W. Porges, Accuracy of the LifeShift® (Vivometrics) in the detection of cardiac rhythms, Biological Psychology. 75 (2007) 300–305. doi:10.1016/j.biopsycho.2007.04.001.

[279] V. Parsonnet, J. Driller, D. Cook, S.A. Rizvi, Thirty-One Years of Clinical Experience with "Nuclear-Powered" Pacemakers, Pacing and Clinical Electrophysiology. 29 (2006) 195–200. doi:10.1111/j.1540-8159.2006.00317.x.

[280] Thermoelectric Generator - Global Market Outlook (2016-2022), STRATISTICS Market Research Consulting, Gaithersburg, MD, USA, 2017. http://www.strategymrc.com/report/thermoelectric-generator-market/ (accessed September 6, 2018).

**Maciej HARAS** was born in Gdańsk, Poland in 1984. Received the M.Eng diploma in power electronics from the Gdańsk University of Technology and the Polytechnique de Grenoble (2008). He obtained a Ph.D. in nanotechnology from the Université Lille-1 (2016), investigating silicon-based thermoelectric generators. This work was awarded with the best Ph.D. dissertation prize from the Université Catholique de Lille.

He joined STMicroelectronics R&D (2011) working on energy harvesting. In 2014 he joined IEMN laboratory and engaged there in development of CMOS compatible thermoelectric generators and mechanical characterization of silicon nanowires. Currently he is the principal scientist at the CEZAMAT laboratory.

**Thomas SKOTNICKI** was with France Telecom from 1985 till 1999 when he joint STMicroelectronics. He became the first STMicroelectronics Company Fellow and Technical Vice-President. He invented the UTBB FDSOI structure (in production at STMicroelectronics, GF and Samsung). Today he is Director of CEZAMAT Consortium and Professor at Warsaw University of Technology, Poland. He holds 80 patents and has authored close to 400 scientific papers, and several book chapters on CMOS and Energy Harvesting. He is an IEEE Fellow, has supervised 29 PhD theses, served as Editor for IEEE TED, and was on JJ Ebers and Frederik Philips IEEE Award Committees.



## HIGHLIGHTS

- Internet of Things market quantification, future growth and needs identified
- Energy harvesting methods hierarchy and their common performance presented
- Fossil fuels and heat losses availability, quantification and reserves highlighted
- Scientific/commercial thermoelectric topologies, materials and performance reviewed
- Performance of energy management circuits for thermo-generators compared

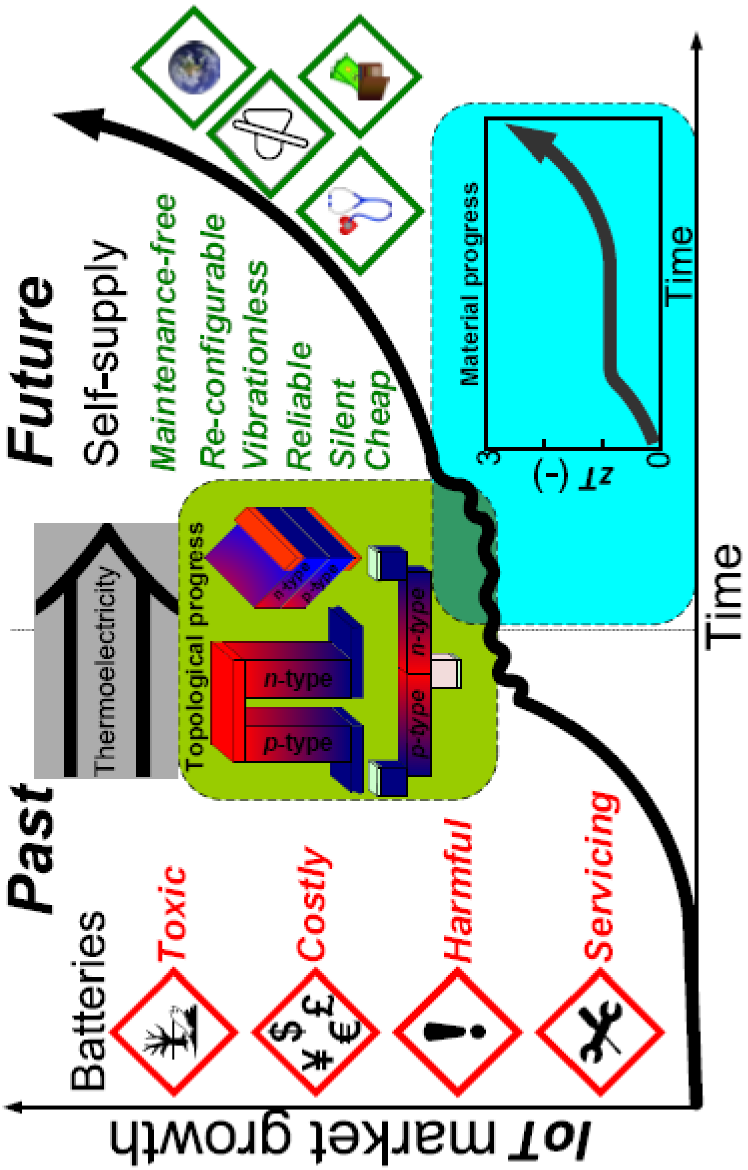
IoT market growth
Time
Batteries
Past
Toxic
Costly
Harmful
Servicing
Thermoelectricity
Topological progress
n-type
p-type
Future
Self-supply
Maintenance-free
Re-configurable
Vibrationless
Reliable
Silent
Cheap
Material progress
zT (-)
3
0
Time